AIR FORCE REPORT NO.
SAMSO-TR-72-178

AEROSPACE REPORT NO.
TR-0073(3404)-1

AD 745577

1.8:1 Bandwidth UHF 3 × 3 Array of Crossed Open-Sleeve Dipoles

Prepared by H. E. KING and J. L. WONG
Electronics Research Laboratory
Laboratory Operations

72 JUN 30

Systems Engineering Operations
THE AEROSPACE CORPORATION

Prepared for SPACE AND MISSILE SYSTEMS ORGANIZATION
AIR FORCE SYSTEMS COMMAND
LOS ANGELES AIR FORCE STATION
Los Angeles, California

Reproduced by
NATIONAL TECHNICAL
INFORMATION SERVICE
U S Department of Commerce
Springfield VA 22151

APPROVED FOR PUBLIC RELEASE:
DISTRIBUTION UNLIMITED

DDC
RECEIVED
JUL 28 1972
B

UNCLASSIFIED

Security Classification

DOCUMENT CONTROL DATA - R & D

(Security classification of title, body of abstract and indexing annotation must be entered when the overall report is classified)

1. ORIGINATING ACTIVITY *(Corporate author)* The Aerospace Corporation El Segundo, California	2a. REPORT SECURITY CLASSIFICATION Unclassified 2b. GROUP

3. REPORT TITLE

1.8:1 BANDWIDTH UHF 3 X 3 ARRAY OF CROSSED OPEN-SLEEVE DIPOLES

4. DESCRIPTIVE NOTES *(Type of report and inclusive dates)*

5. AUTHOR(S) *(First name, middle initial, last name)*

Howard E. King and Jimmy L. Wong

6. REPORT DATE 72 JUN 30	7a. TOTAL NO. OF PAGES 49	7b. NO. OF REFS 4
8a. CONTRACT OR GRANT NO. F04701-72-C-0073 b. PROJECT NO. c d	9a. ORIGINATOR'S REPORT NUMBER(S) TR-0073(3404)-1 9b. OTHER REPORT NO(S) *(Any other numbers that may be assigned this report)* SAMSO-TR-72-178	

10. DISTRIBUTION STATEMENT

Approved for public release; distribution unlimited

11. SUPPLEMENTARY NOTES	12. SPONSORING MILITARY ACTIVITY Space and Missile Systems Organization Air Force Systems Command Los Angeles, California

13. ABSTRACT

A circularly polarized nine-element (3 X 3) planar array antenna system has been evaluated for use on a synchronous satellite. The array elements are mounted on a 104-in. square reflector, and the basic radiating element is a crossed open-sleeve dipole with good VSWR and pattern characteristics over a 1.8:1 frequency band (225 to 400 MHz). The electrical performance of the antenna was measured using a half-scale model. It is shown that the antenna can provide an EOE gain (gain in the direction of the edge-of-the-earth) of greater than 14 dB from 225 to 250 MHz and greater than 11 dB from 250 to 400 MHz, based on the results of the half-scale model measurements. The measured axial ratio is less than 1.6 dB throughout the entire operating frequency band.

Details of illustrations in this document may be better studied on microfiche

Ia

DD FORM (FACSIMILE) 1473

UNCLASSIFIED

Security Classification

14. KEY WORDS

Open-sleeve dipoles
Planar array
Synchronous satellite antenna

Distribution Statement (Continued)

Abstract (Continued)

Ib

Air Force Report No.
SAMSO-TR-72-178

Aerospace Report No.
TR-0073(3404)-1

1.8:1 BANDWIDTH UHF 3 × 3 ARRAY OF CROSSED OPEN-SLEEVE DIPOLES

Prepared by

H. F. KING and J. L. WONG
Electronics Research Laboratory
Laboratory Operations

72 JUN 30

Systems Engineering Operations
THE AEROSPACE CORPORATION

Prepared for

SPACE AND MISSILE SYSTEMS ORGANIZATION
AIR FORCE SYSTEMS COMMAND
LOS ANGELES AIR FORCE STATION
Los Angeles, California

Approved for public release;
distribution unlimited

IC

FOREWORD

This report is published by The Aerospace Corporation, El Segundo, California, under Air Force Contract No. F04701-72-C-0073.

This report, which documents research carried out from July to November 1971, was submitted 6 June 1972 to Colonel Walter W. Sanders, SK, for review and approval.

The authors wish to thank H. F. Meyer and P. J. Parszik for their interest and support of this study. Thanks also go to D. G. Coder, M. E. Schwartz, and C. Romero for their technical assistance, to J. T. Shaffer and O. L. Reid for testing the antenna, and to D. S. Chang for the computer programming.

Approved

A. H. Silver, Director
Electronics Research Laboratory
Laboratory Operations

H. F. Meyer, Systems Engineering Director
Tactical Satellite Communications Programs
Satellite Systems Division
Systems Engineering Operations

Publication of this report does not constitute Air Force approval of the report's findings or conclusions. It is published only for the exchange and stimulation of ideas.

WALTER W. SANDERS, Col, USAF
Deputy for Space
Communications Systems

ABSTRACT

A circularly polarized nine-element (3 × 3) planar array antenna system has been evaluated for use on a synchronous satellite. The array elements are mounted on a 104-in. square reflector, and the basic radiating element is a crossed open-sleeve dipole with good VSWR and pattern characteristics over a 1.8:1 frequency band (225 to 400 MHz). The electrical performance of the antenna was measured using a half-scale model. It is shown that the antenna can provide an EOE gain (gain in the direction of the edge-of-the-earth) of greater than 14 dB from 225 to 250 MHz and greater than 11 dB from 250 to 400 MHz, based on the results of the half-scale model measurements. The measured axial ratio is less than 1.6 dB throughout the entire operating frequency band.

CONTENTS

FOREWORD ii

ABSTRACT iii

I. INTRODUCTION 1

II. DESCRIPTION OF ANTENNA SYSTEM 3

III. RESULTS 9

A. Computed Patterns and Directivity 9

B. Measured Data 16

1. Feed Network Characteristics 16

2. VSWR 19

3. Radiation Patterns 22

4. Directivity and Gain 32

5. Axial Ratio 41

IV. SUMMARY AND CONCLUSIONS 43

REFERENCES 45

Preceding page blank

FIGURES

1. Overall View of 3 × 3 Crossed Open-Sleeve Dipole Planar Array 4

2. Close-Up View of Crossed Open-Sleeve Dipole Assembly 5

3. Crossed, Flat Open-Sleeve Dipole Model 6

4. Schematic Diagram of Array Feed Network 8

5. Measured Element Patterns for Dipole-to-Reflector Spacings of 4.31 and 5 in. 10

6. Array Geometry 11

7. Computed Array Patterns for Element Spacing of 16 in. and Dipole-to-Reflector Spacing of 5 in. 12

8. Computed Array Patterns for Element Spacing of 16 in. and Dipole-to-Reflector Spacing of 4.31 in. 13

9. Computed Array Patterns for Element Spacing of 18 in. and Dipole-to-Reflector Spacing of 4.31 in. 14

10. Computed Directivities for Dipole-to-Reflector Spacings of 4.31 and 5 in. 15

11. Feed Network Loss Characteristics 17

12. VSWR of Single Element, Elements Embedded in Array, and Complete Array for Dipole-to-Reflector Spacing of 5 in. and Element Spacing of 16-in. 20

13. VSWR of Single Element and Complete Array for Dipole-to-Reflector Spacing of 4.31 in. and Element Spacings of 16 and 18 in. 21

14. Mismatch Losses for 4.31- and 5-in. Dipole-to-Reflector Spacings 22

FIGURES (Continued)

15. Measured Radiation Patterns for Element Spacing of 16 in. and Dipole-to-Reflector Spacing of 4.31 in. with Rotating Linearly Polarized and Circularly Polarized Illumination 24

16. Measured Radiation Patterns with Expanded Abscissa Scale, Using a Rotating Linearly Polarized Source 29

17. Comparison of Measured and Computed Radiation Pattern Characteristics for Element Spacing of 16 in. and Dipole-to-Reflector Spacing of 5 in. 33

18. Comparison of Measured and Computed Radiation Pattern Characteristics for Element Spacing of 16 in. and Dipole-to-Reflector Spacing of 4.31 in. 35

19. Comparison of Measured and Computed Radiation Pattern Characteristics for Element Spacing of 18 in. and Dipole-to-Reflector Spacing of 4.31 in. 36

20. Comparison of Directivity Determined from Computed Patterns and Measured Patterns for the Planar Array 37

21. Comparison of Measured and Predicted Gain for Three Planar Array Configurations 39

22. Measured Axial Ratios at the Beam Peak for Three Planar Array Configurations 42

I. INTRODUCTION

This report describes the results of a theoretical and experimental evaluation of a wideband UHF planar array of crossed open-sleeve dipoles. This array is a candidate antenna configuration for a communication satellite at synchronous altitude operating in the 225 to 400 MHz (1.8:1 bandwidth) frequency range. The primary objective of this study was to establish the antenna gain at an off-axis angle of 8.65 deg from the beam peak. This angle corresponds to a line-of-sight to the edge-of-the-earth (EOE) from a synchronous orbit satellite. The EOE gain represents an important factor in the system analysis of the communication link.

The experimental work was done with a half-scale model (450 to 800 MHz), and all the results are reported with reference to the scaled dimensions. The array consists of nine elements (3 × 3 configuration) of crossed open-sleeve dipoles (Ref. 1) mounted on a 52-in. square reflector. The orthogonal dipoles are fed in phase quadrature to acquire circular polarization. Sleeve dipoles were selected to attain the desired bandwidth. The dipole-to-reflector spacing and the distance between elements were varied during the investigation. The dipole configurations and spacings were selected to optimize the array performance in the 225 to 300 MHz (450 to 600 MHz, half-scale) band without substantial degradation of antenna gain at the upper frequencies.

The element patterns used for the array pattern and directivity computations are discussed. Measured antenna gain and patterns are compared with the computed results. The measured VSWR of the individual dipoles and the array of dipoles are also included in the report.

II. DESCRIPTION OF ANTENNA SYSTEM

The frequency of operation for the half-scale model is from 450 to 800 MHz. There are no strict requirements on the antenna beam shape and sidelobe levels, but the off-axis (±8.65 deg from beam peak) gain is to be maximized. Circular polarization is required.

The array consists of nine crossed open-sleeve dipoles arranged in a square grid as shown in the photograph of Fig. 1. The elements are fed by a corporate feed structure and are uniformly excited. The reflector is 52-in. square and is fabricated with 1/2-in. square mesh wire screen.

To achieve wideband impedance and pattern performance, open-sleeve dipoles (Refs. 1, 2) were used. The VSWR is less than 2.5:1 over the 225 to 400 MHz band. Sleeve antennas generally have wider pattern bandwidth characteristics than a conventional cylindrical (fat) dipole (Ref. 3). The dipoles and sleeves are constructed with solid metallic surfaces, although they could have been constructed in a wire-grid arrangement to minimize weight (Ref. 2). A close-up view of the dipole assembly is shown in Fig. 2.

The original open-sleeve antenna reported by Barkley (Ref. 4) consisted of a dipole with two closely spaced parasitic elements, the length of the parasites (sleeves) being approximately one-half that of the center-fed dipole. Experimental studies of the open-sleeve antenna (Ref. 1) revealed that the sleeves could have a wide variety of configurations without any degradation to the VSWR response. For simplicity in construction of the crossed dipole antennas, a flat sleeve arrangement was chosen. Figures 1 and 2 show the flat metal sleeve construction and the Styrofoam support for the sleeves.

Figure 3 shows the construction details of the crossed open-sleeve dipoles and balun. A coaxial line was used to feed the dipole, and the antenna structure was made to incorporate a balun. The feed line consisted of a copper-clad, 0.141-in. diam semirigid coaxial cable. The balanced line of the balun was also a length of the semirigid cable, but without the center

Preceding page blank

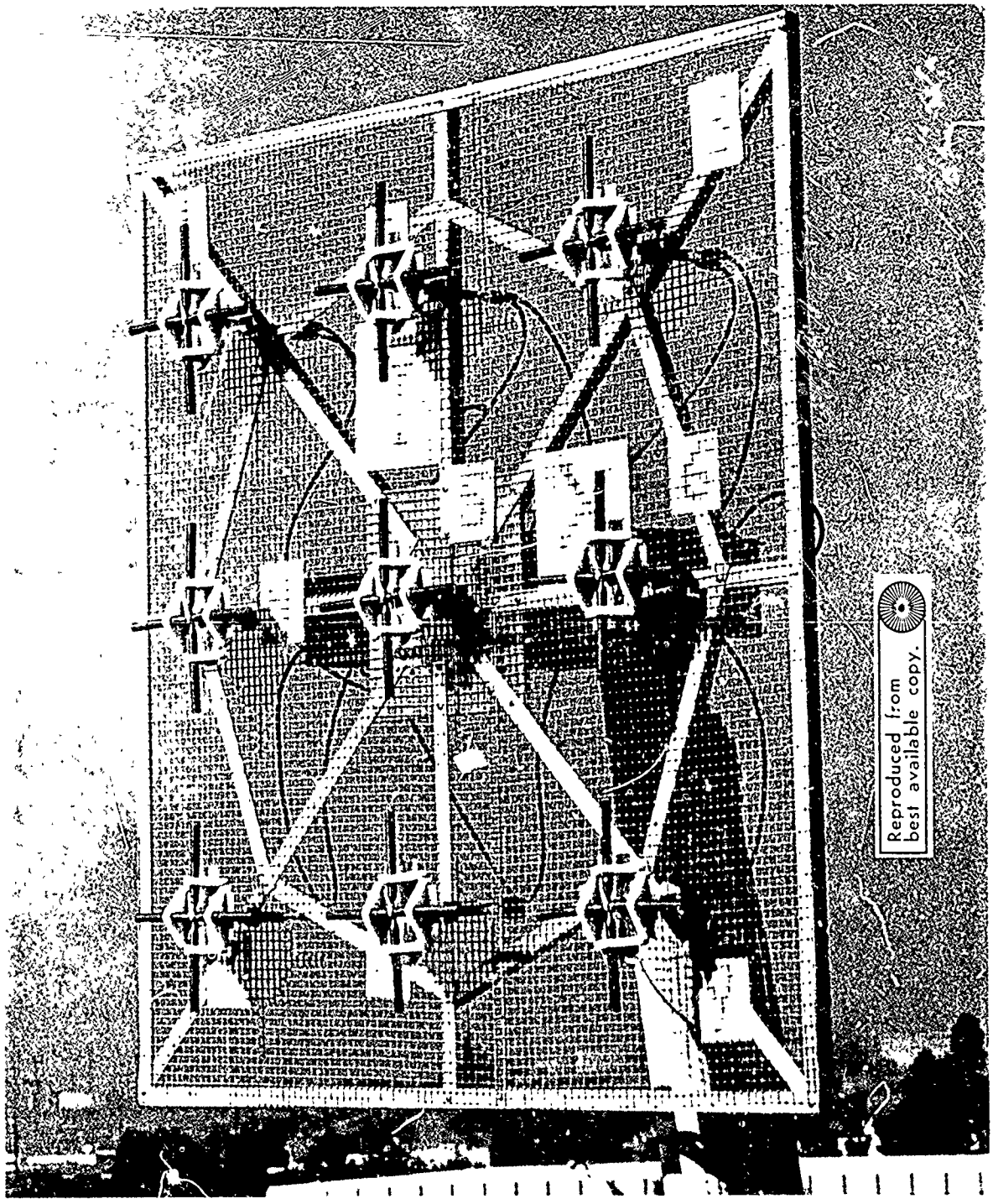

Reproduced from best available copy.

Figure 1. Overall View of 3 × 3 Crossed Open-Sleeve Dipole Planar Array

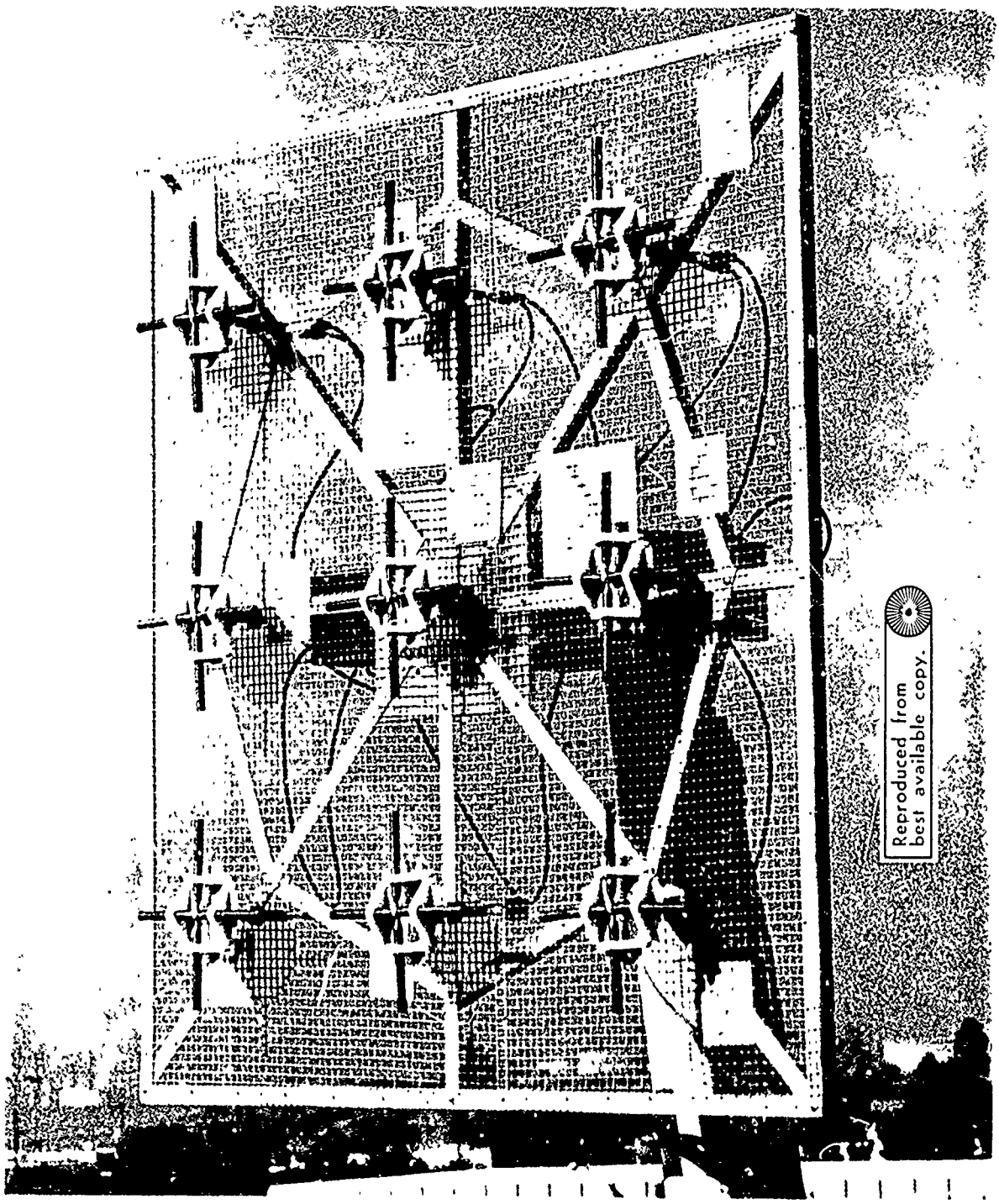

Reproduced from best available copy.

Figure 1. Overall View of 3 × 3 Crossed Open-Sleeve Dipole Planar Array

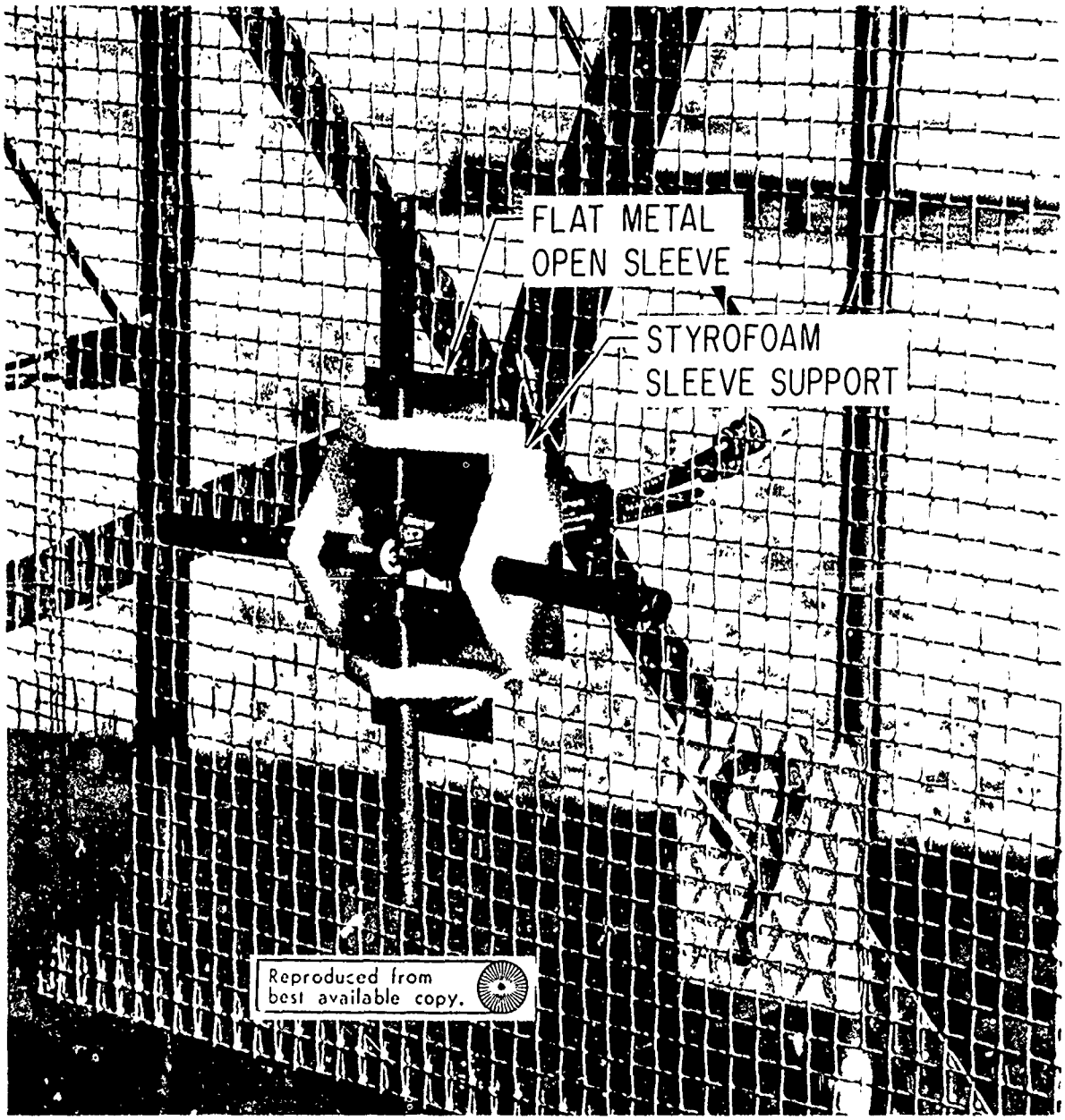

Reproduced from
best available copy.

Figure 2. Close-Up View of Crossed Open-Sleeve Dipole Assembly

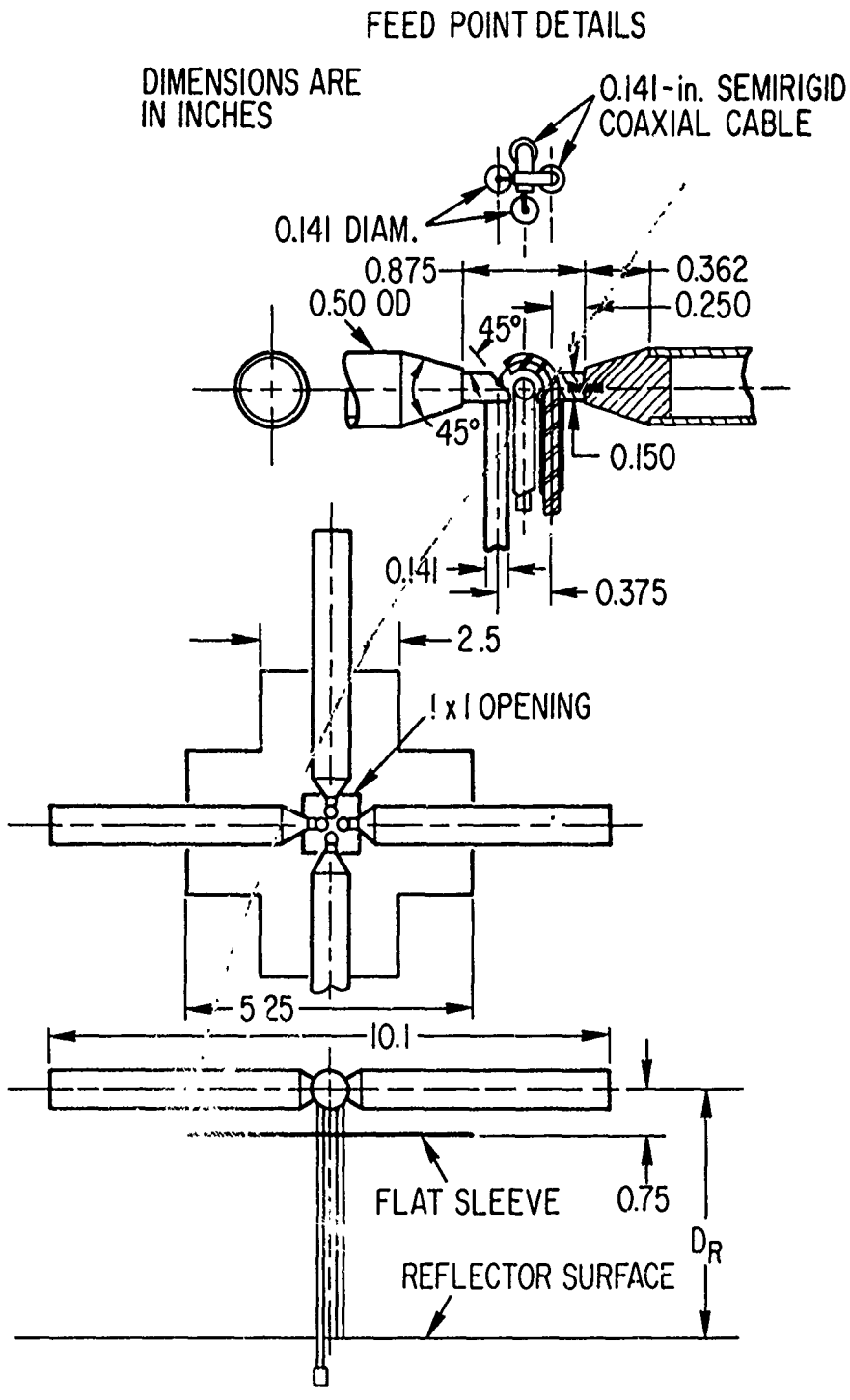

Figure 3. Crossed, Flat Open-Sleeve Dipole Model

conductor, and the short circuit of this line was coincident with the reflector surface. The dipoles were screwed into the feed terminals and the sleeves were supported by Styrofoam.

The array feed network schematic diagram is shown in Fig. 4. Four 3-way power dividers are used to feed the "Y" dipoles and another four to feed the "X" dipoles. The X and Y dipoles are fed in quadrature by a 90-deg hybrid to provide circular polarization.

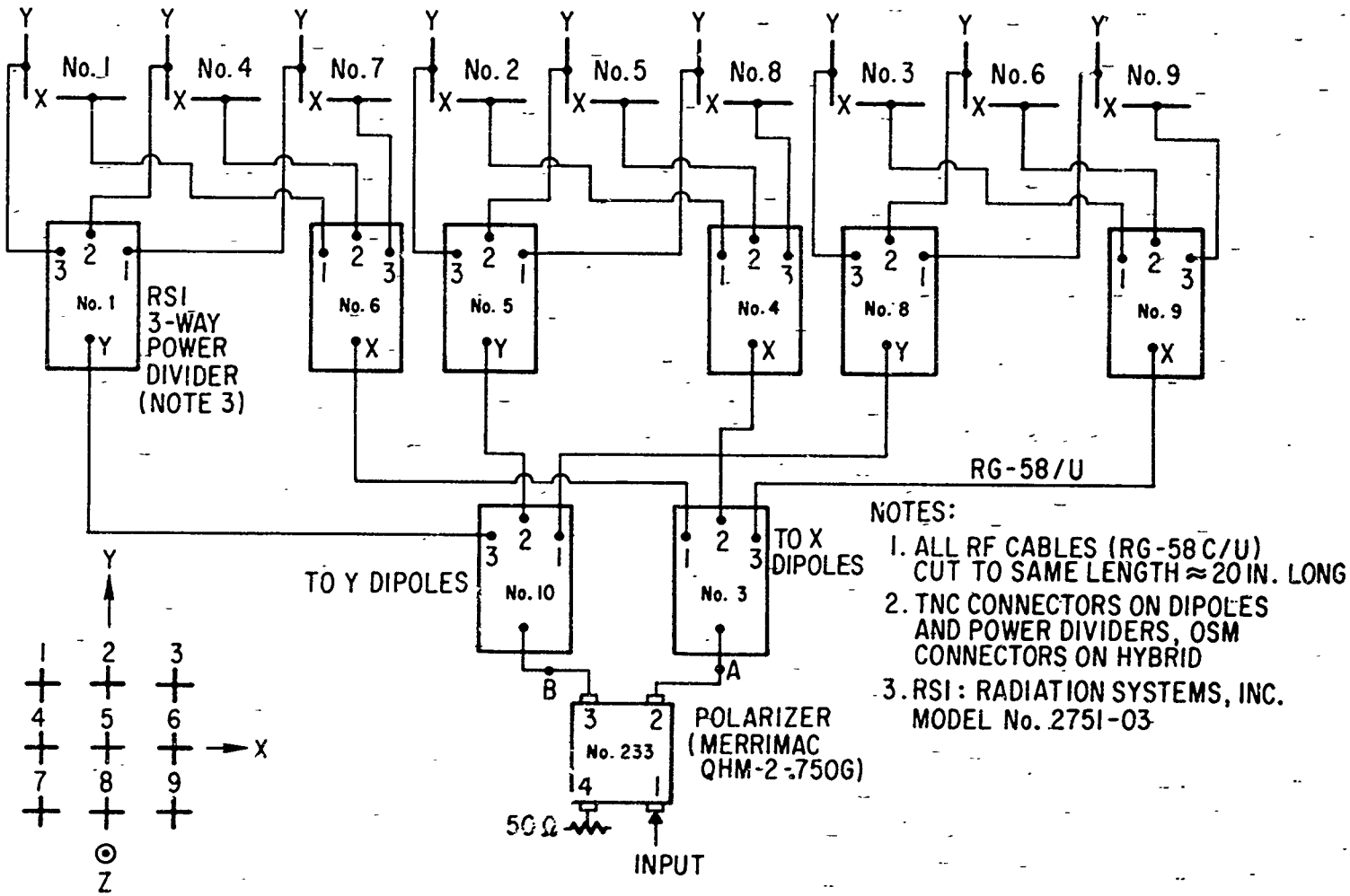

Figure 4. Schematic Diagram of Array Feed Network

III. RESULTS

A. COMPUTED PATTERNS AND DIRECTIVITY

Measured patterns of an isolated element were used for the array pattern computations. A single crossed open-sleeve dipole assembly mounted in the center of a 52-in. square reflector was used to measure the element pattern. E and H plane patterns (linear polarization) were recorded. To derive the response for circular polarization, the RSS of the two measured field components was calculated; i.e.,

$$E_{cp} = \sqrt{E_H^2 + E_E^2}$$

where E_H and E_E are the H and E plane patterns, respectively. The resulting circularly polarized element patterns for 450, 500, 600, 700 and 800 MHz are shown in Fig. 5 for dipole-to-reflector spacings of 4.31 and 5 in. The patterns in the backlobe region ($90 < \theta \leq 180$) are not shown, since they are neglected in the array computations. Mutual coupling effects were also neglected in the array analysis, but they will be considered in a forthcoming companion report.

The coordinate system used for the array analysis is illustrated in Fig. 6. The general equation for the field pattern of an $N \times N$ planar array with uniform distribution may be written as

$$E(\theta, \phi) = E_e(\theta) \frac{\sin\left(N\pi \frac{s}{\lambda} \sin\theta \sin\phi\right)}{N \sin\left(\frac{\pi s}{\lambda} \sin\theta \sin\phi\right)} \cdot \frac{\sin\left(N\pi \frac{s}{\lambda} \sin\theta \cos\phi\right)}{N \sin\left(\frac{\pi s}{\lambda} \sin\theta \cos\phi\right)} \qquad (1)$$

where s is the element spacing, $E_e(\theta)$ is the measured element pattern (from Fig. 5), and θ is measured from the broadside direction of the array. The computed patterns for $N = 3$

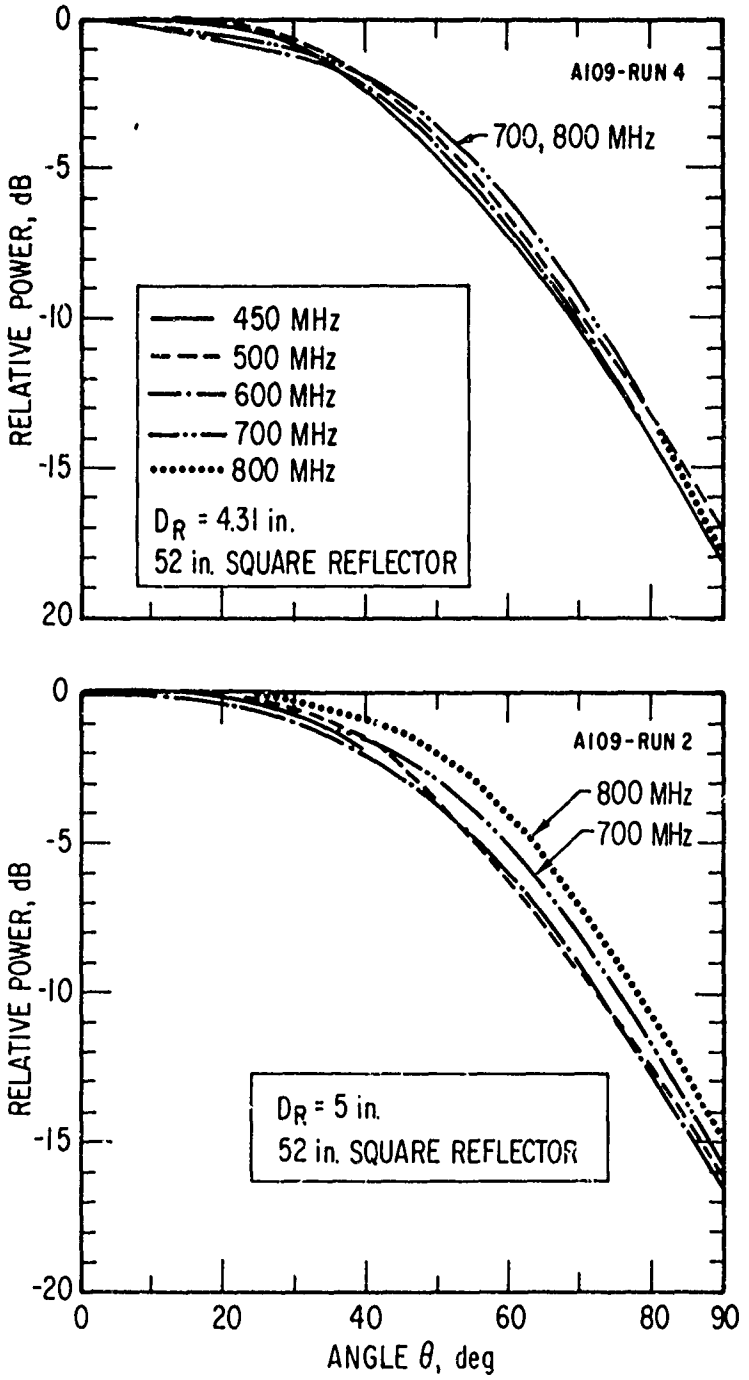

Figure 5. Measured Element Patterns for Dipole-to-Reflector Spacings of 4.31 and 5 in.

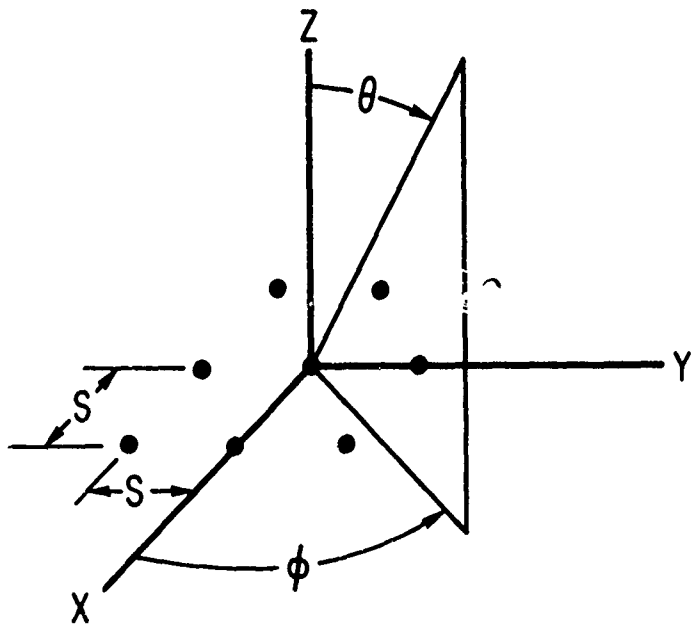

Figure 6. Array Geometry

are plotted in Figs. 7, 8, and 9 for a 5-in. dipole-to-reflector spacing and an element spacing of 16 in. and also for a 4.31-in. dipole-to-reflector spacing with element spacings of 16 and 18 in. Because of symmetry, patterns in the $\phi = 90$ and $\phi = 135$ deg planes are identical to those of the $\phi = 0$ and $\phi = 45$ deg planes, respectively.

The directivity was determined by integration of the power pattern over the visible space ($0 \leq \theta \leq \pi/2$), since the radiation characteristics in the region $\pi/2 < \theta < \pi$ are not known. The directivity is expressed as

$$D = \frac{4\pi}{\int_0^{2\pi}\int_0^{\pi/2} E^2(\theta, \phi) \sin\theta \, d\theta \, d\phi} \tag{2}$$

Figure 10 shows the peak directivity and the EOE directivity values as functions of frequency for dipole-to-reflector spacings of 4.31 and 5 in. with

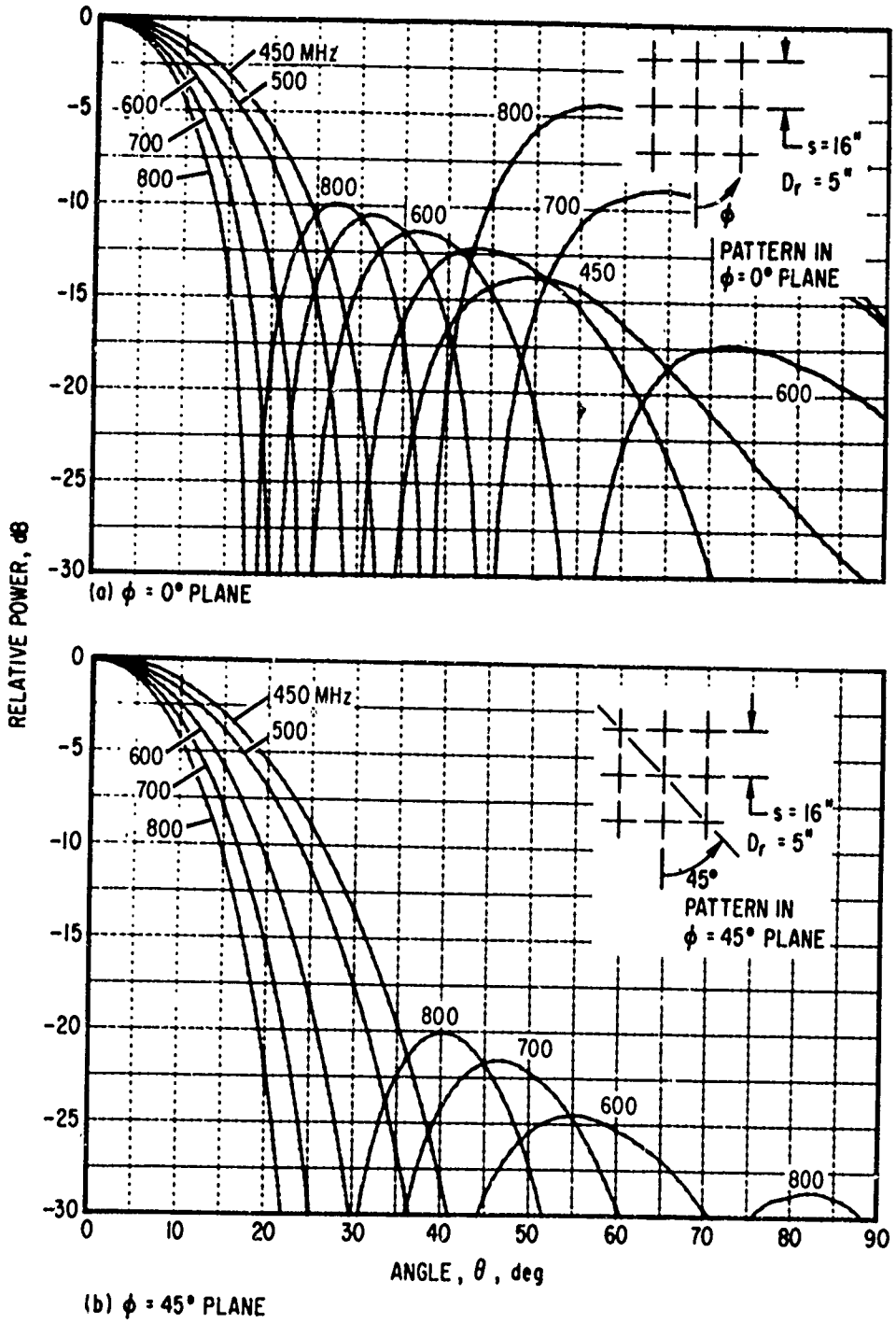

Figure 7. Computed Array Patterns for Element Spacing of 16 in. and Dipole-to-Reflector Spacing of 5 in.

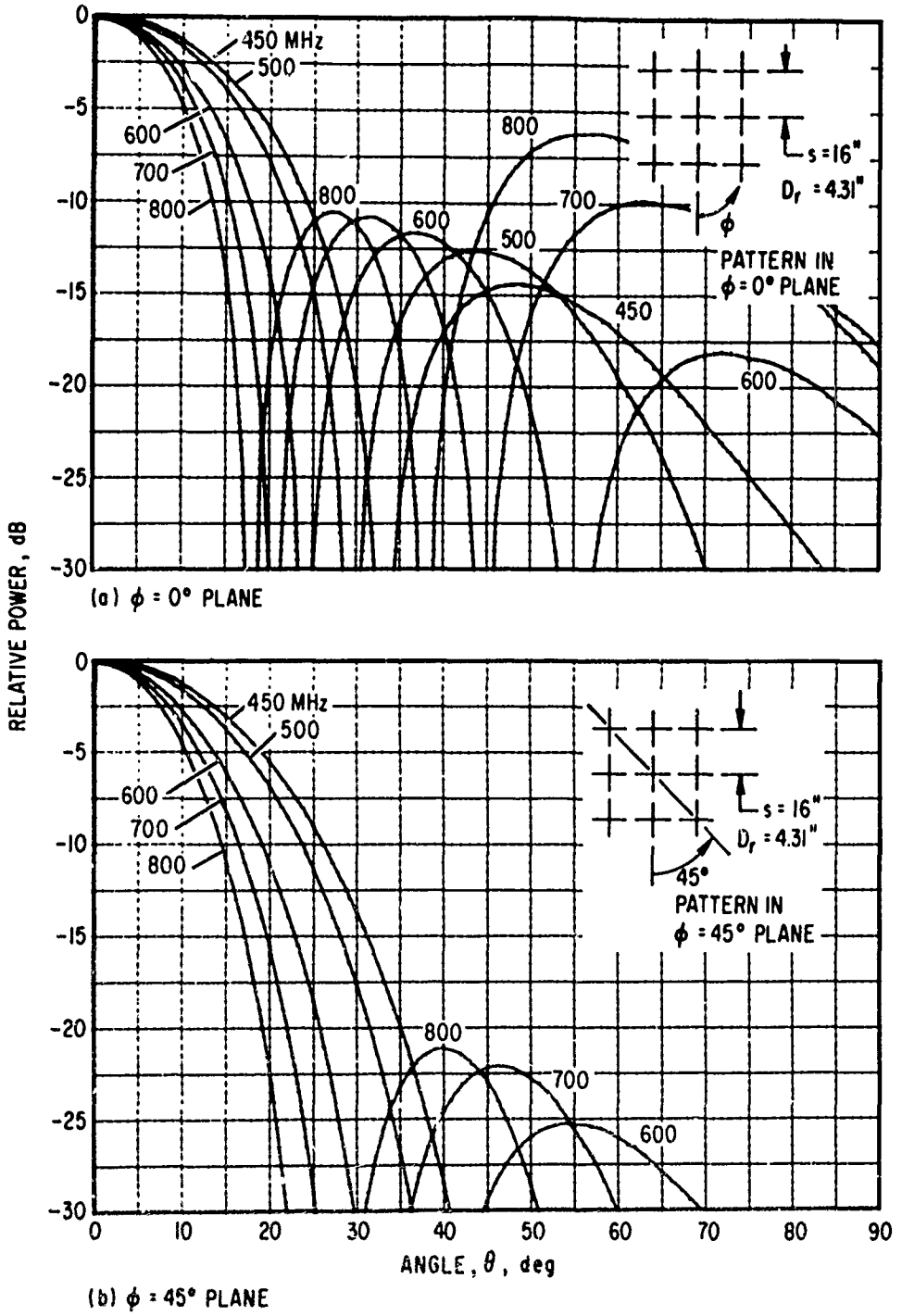

Figure 8. Computed Array Patterns for Element Spacing of 16 in. and Dipole-to-Reflector Spacing of 4.31 in.

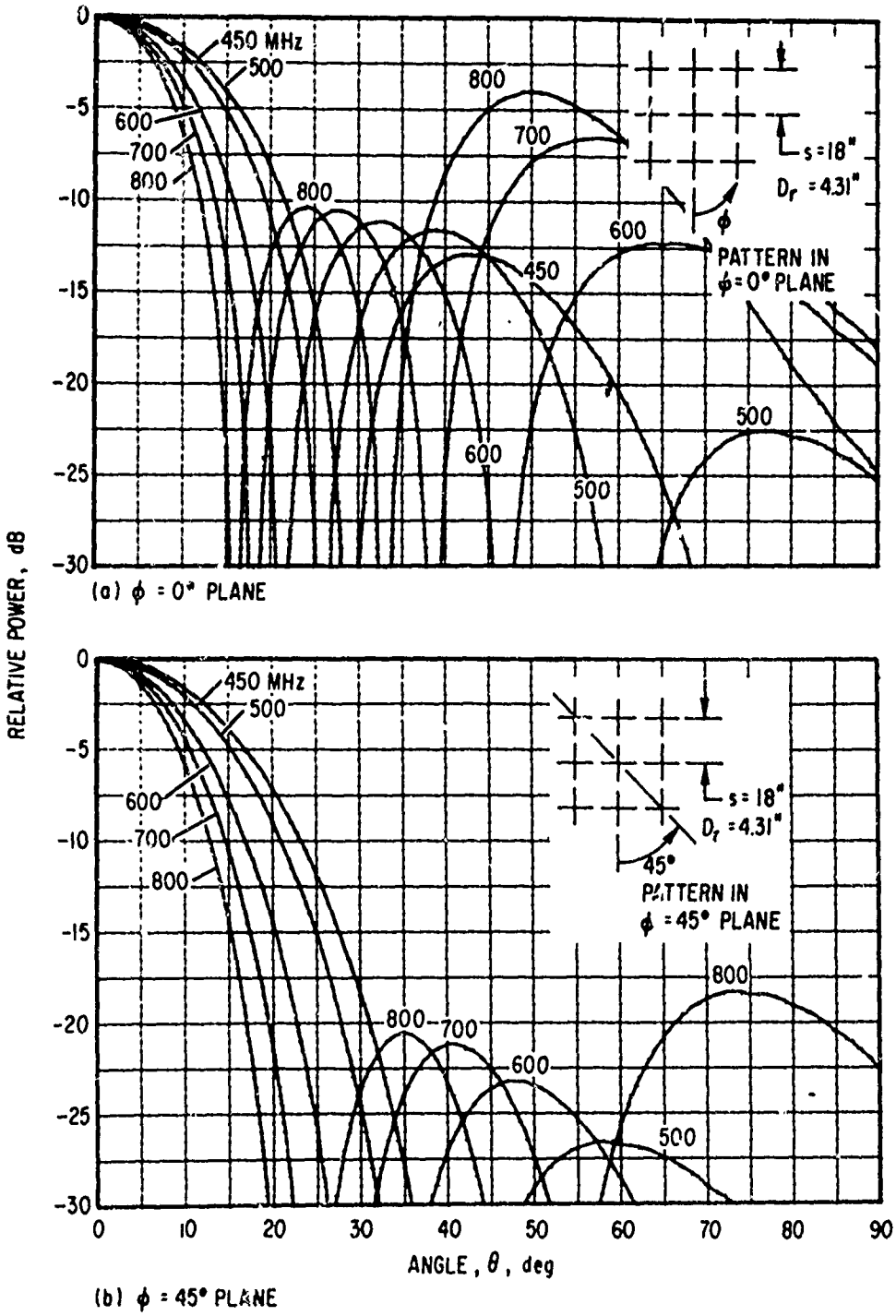

Figure 9. Computed Array Patterns for Element Spacing of 18 in. and Dipole-to-Reflector Spacing of 4.31 in.

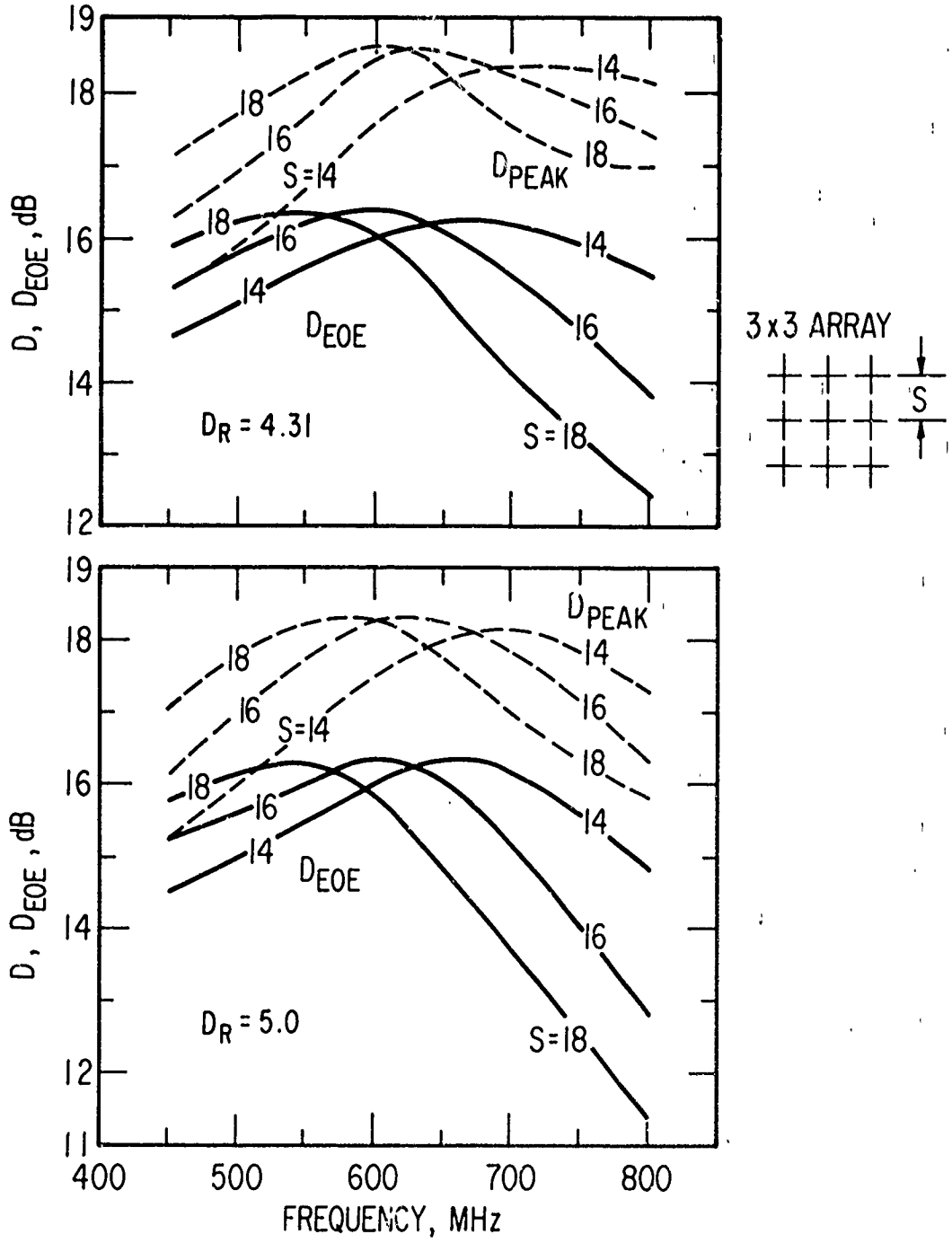

Figure 10. Computed Directivities for Dipole-to-Reflector Spacings of 4.31 and 5 in.

the element spacing as a parameter. At the low end of the frequency band, the directivities are essentially the same for the two dipole-to-reflector spacings. At 800 MHz, the 4.31-in. spacing provides an enhanced directivity of approximately 1 dB. This was expected, because the 4.31-in. spacing corresponds to 0.29λ at 800 MHz and is the position where the radiation pattern beam bifurcation begins to become noticeable. At 5-in. dipole-to-reflector spacing, the spacing is 0.34λ and beam splitting definitely exists, resulting in a lower element directivity and thus a lower array directivity.

The directivity represents the gain of an antenna with no losses, and the actual gain of the planar array is determined by subtracting out the various losses. The measured feed network, polarizer, and mismatch losses are presented in Section III-B. The antenna ohmic, balun, and other unknown losses cannot be measured directly and are inferred from the difference between the computed and measured gain values.

For the 3 × 3 array, a 16-in. element spacing provides optimum EOE directivity (> 15.2 dB) in the frequency range of 450 to 700 MHz; however, at 800 MHz, the EOE directivity drops to 13.9 and 12.9 dB for the dipole-to-reflector spacings of 4.31 and 5 in., respectively. With an element spacing of 18 in., the EOE gain at the low end of the frequency band may be enhanced by about 0.5 dB but only at the expense of a gain degradation of about 1.5 dB at the high end of the band. A 14-in. element spacing provides a more uniform EOE directivity, as compared to s = 16 and 18, but the overall directivity is lower, particularly in the more important 450 to 600 MHz band.

B. MEASURED DATA

1. FEED NETWORK CHARACTERISTICS

The measured losses of the feed network (Fig. 4) and its individual components are shown in Fig. 11. The circles represent data points, and the dashed-straight line is a least squares fit to the data points with the standard deviation, s_d.

Figure 11(a) shows the overall losses of three cascaded lengths of RG-58C/U cable, each approximately 20-in. long, complete with TNC connectors. These connector-cable assemblies, as used in the feed network,

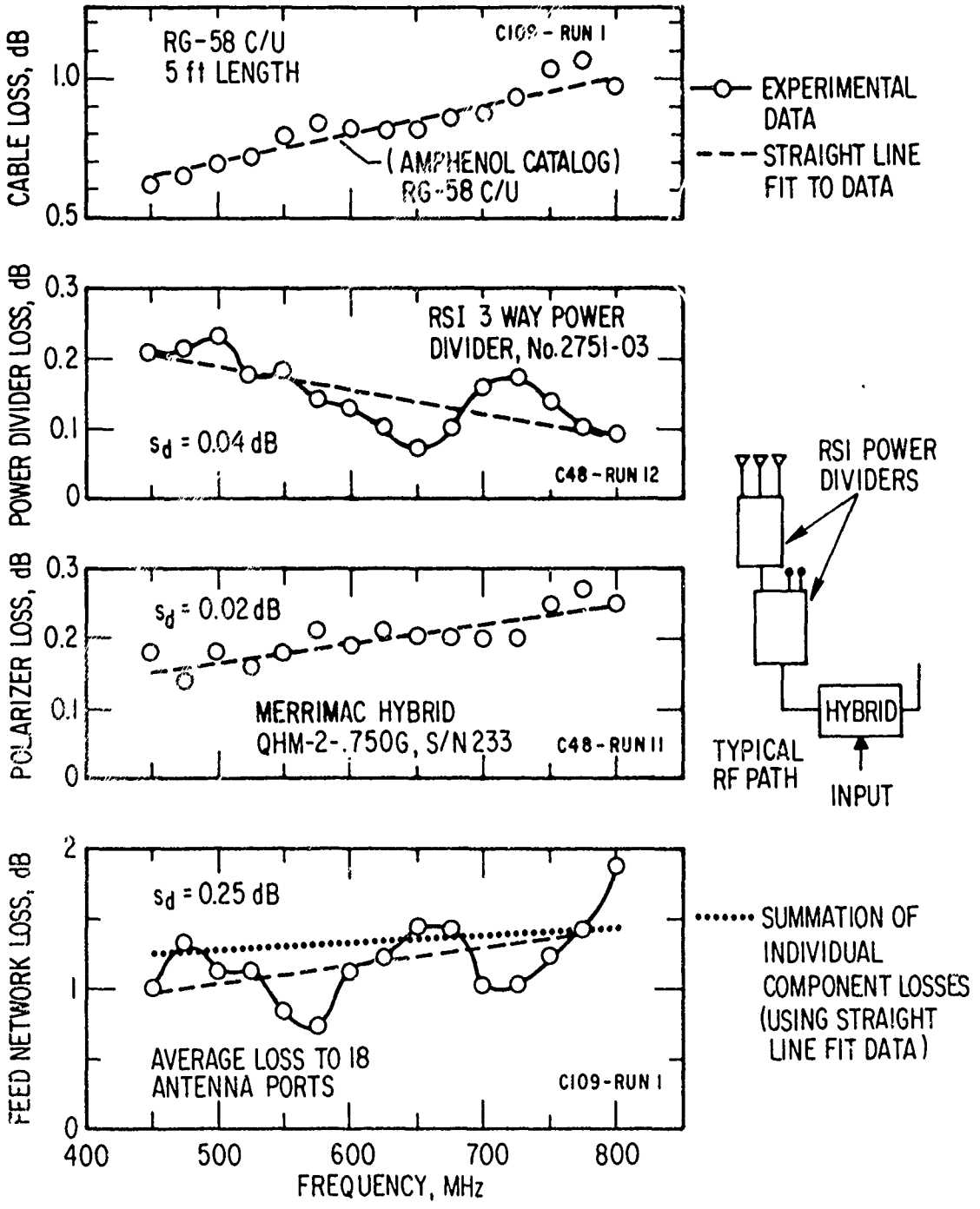

Figure 11. Feed Network Loss Characteristics

have an overall length of 5 ft. The cable losses for a 5-ft length of RG-58C/U cable, as given in the Amphenol catalog, are also shown for comparison.

The Radiation Systems, Inc. (RSI) 3-way power divider losses shown in Fig. 11(b) represent the average of the three output ports and the average of eight units. The stripline units have an average insertion loss of less than 0.22 dB. The maximum deviation among the power dividers was less than ±0.2 dB. From port-to-port for the same unit, the deviations were less than ±0.1 dB. The phase deviation between each port for a single unit was less than 0.1 deg.

The insertion loss of the polarizer is the average of the losses at the two output ports. The compact unit with OSM connectors has an insertion loss of less than 0.27 dB. The differential phase from 90 deg between the two ports was less than 0.6 deg and, as an average, less than 0.2 deg over the frequency range. The power imbalance between the two output ports is given in Section III-B(5). The performance of the hybrid was satisfactory at 450 MHz, even though the unit was advertised by the manufacturer for operation in the 500 to 1000 MHz frequency range.

Figure 11(c) shows the overall loss of the feed network from the polarizer input to the antenna-balun ports. The data represent the average for the 18 output ports. The maximum deviation among the ports was ±0.3 dB. The standard deviation of the regression line is 0.25 dB. When summing up the losses of the individual components that comprise the feed network, the total loss is usually represented by a straight line such as the regression line. The deviations from a straight line are caused by the unpredictable mismatch effects and other unknown factors. As a comparison, the regression lines of each of the individual components were summed, with the result as shown by the dotted line of Fig. 11(d). There is a reasonable agreement with the experimental regression line. The differential phases among the 18 output ports were less than 5.8 deg, which is an indication of how well the cables were cut to identical lengths. As an average, the differential phase from 90 deg between the X and Y dipole ports was less than 1 deg. The power imbalance between

the X and Y dipole balun ports was essentially the same as that of the hybrid outputs, which will be evident from the axial ratio discussion (Section III-B(5)).

2. VSWR

The VSWR of a single isolated dipole, the dipoles embedded in the 3 × 3 array, and the inputs to the 3-way power dividers and to the polarizer were measured prior to making any pattern and gain measurements. The results for a dipole-to-reflector spacing of 5 in. and with a 16-in. element spacing are shown in Fig. 12. The VSWR of one isolated dipole is less than 2.3:1. Both the X and Y dipoles of elements No. 5, 7, and 8 (see Fig. 4) were measured at the balun input port, with the remaining elements terminated in 50-ohm loads. These three elements were chosen for the measurements because they have different neighboring dipole arrangements, and the VSWR characteristics would provide an indication of mutual coupling and reflector-edge effects. Rather than plot each curve individually, the maximum spread in the VSWR values is shown (Fig. 12(b)).

Since the X and Y dipoles in the array were fed with separate sets of power dividers, the input VSWR to each set (Ports A and B, respectively, Fig. 4) was measured. The results are shown in Fig. 12(c). The VSWR response is considered good. The VSWR measured at the input of the polarizer with all the dipoles connected is shown by the dotted line. This VSWR is low, as expected, since most of the reflected energy is dissipated in the fourth port of the 90-deg hybrid.

Figure 13 shows the VSWR characteristics for a dipole-to-reflector spacing of 4.31 in. and element spacings of 16- and 18-in. The maximum VSWR of a single dipole is 2.8:1. It should be pointed out that the VSWR can be significantly reduced by making the dipoles fatter and by varying the sleeve parameters, as discussed in Ref. 1. For the purposes of this study, the change in diameter was not considered necessary. The VSWR at the input to the power divider network feeding the X and Y dipoles for element spacings of 16 and 18 in. are shown in Figs. 13(b) and 13(c), respectively.

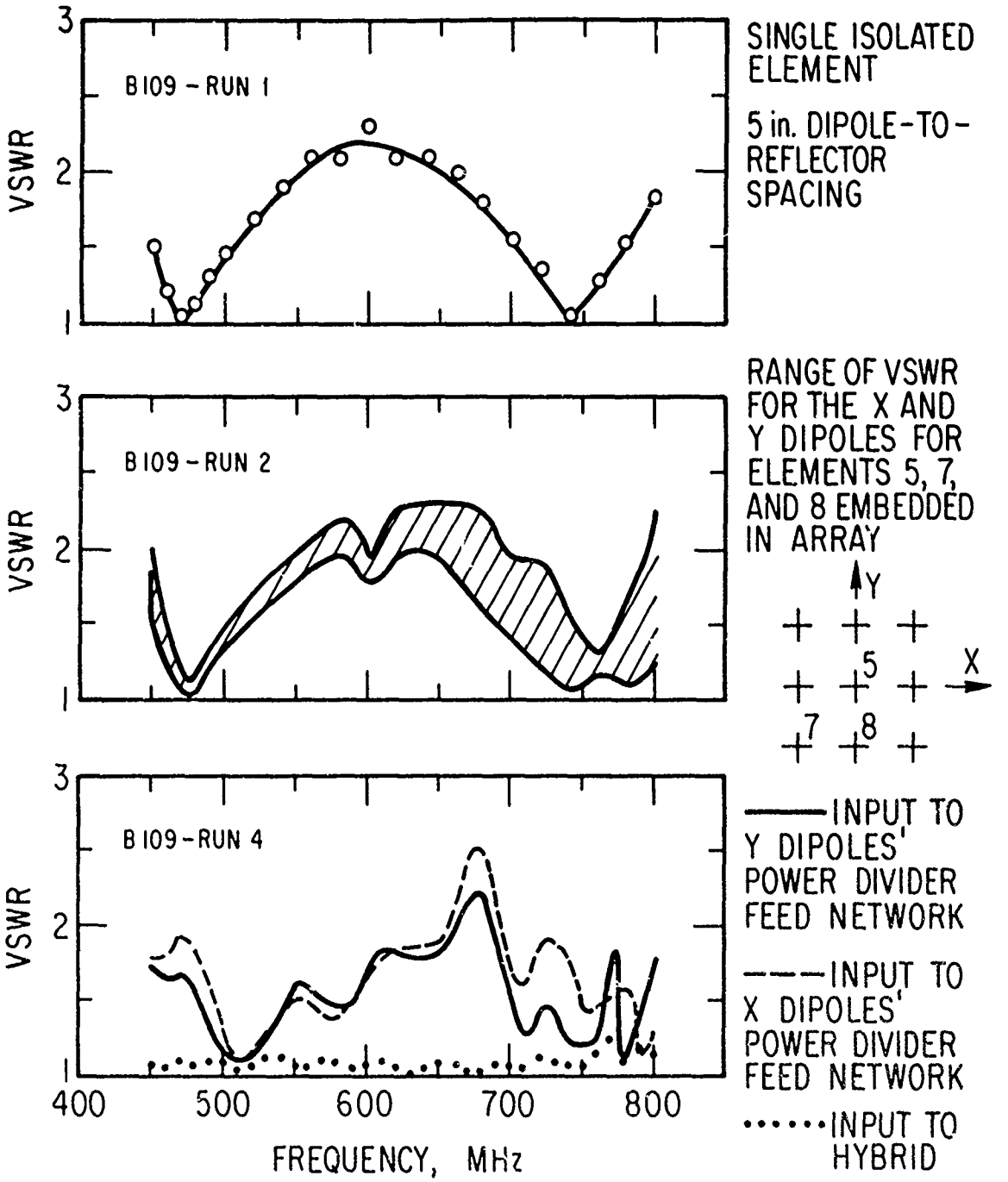

Figure 12. VSWR of Single Element, Elements Embedded in Array, and Complete Array for Dipole-to-Reflector Spacing of 5 in. and Element Spacing of 16-in.

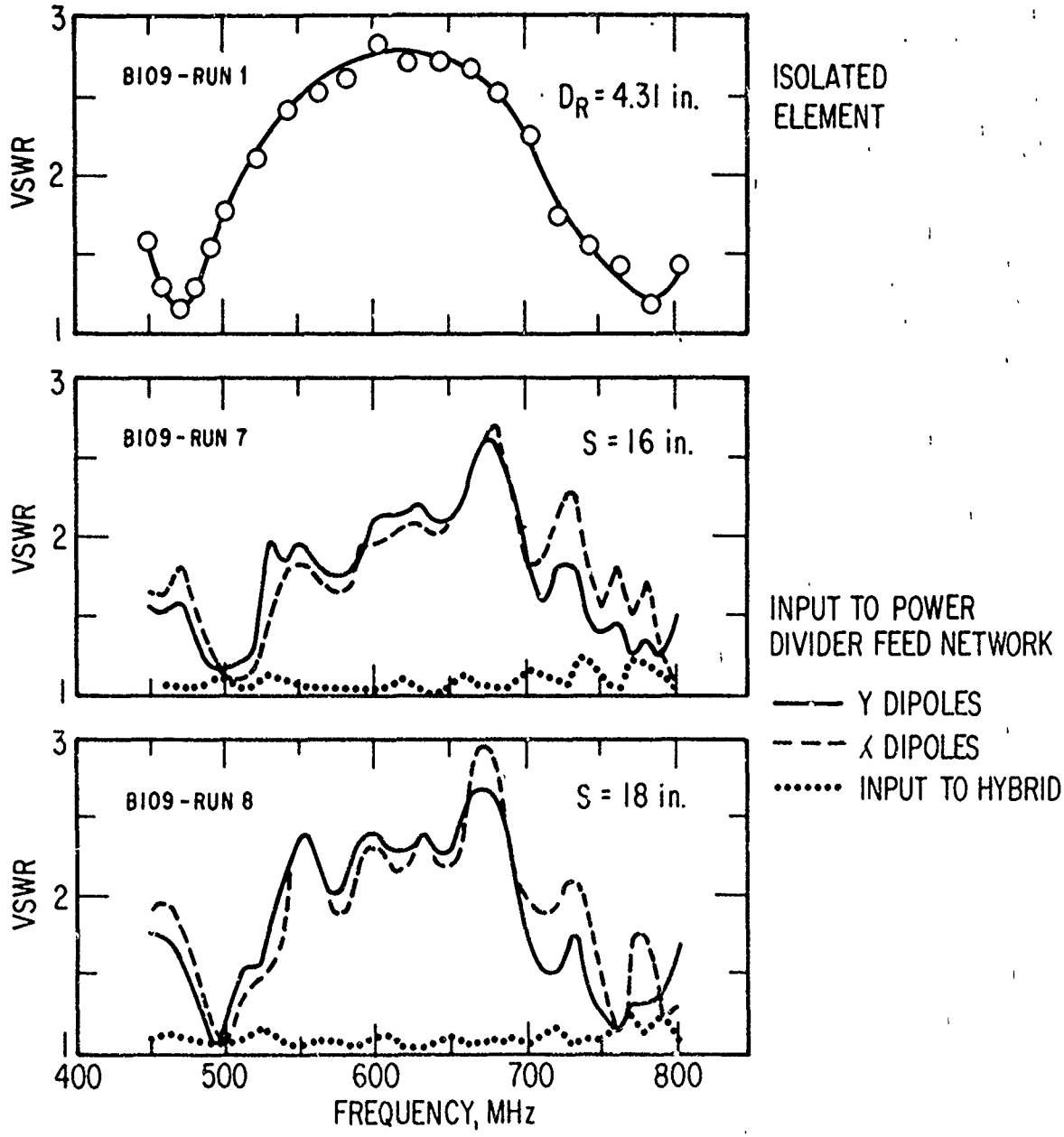

Figure 13. VSWR of Single Element and Complete Array for Dipole-to-Reflector Spacing of 4.31 in. and Element Spacings of 16 and 18 in.

The power loss due to the VSWR, which is not transmitted by the antenna system, is referred to as the mismatch loss. The exact mismatch loss for the array is difficult to determine from the VSWR data. However, for purposes of the present study, the VSWR of a single isolated element was used to determine the mismatch losses. In this manner, the effects resulting from the interactions between the various components in the feed network and the array are not accounted for, but from an examination of Figs. 12 and 13 it appears that this error is quite small. Figure 14 depicts the mismatch losses for the dipole-to-reflector spacings of 4.31 and 5 in., which are used to determine the array gains from the computed directivities.

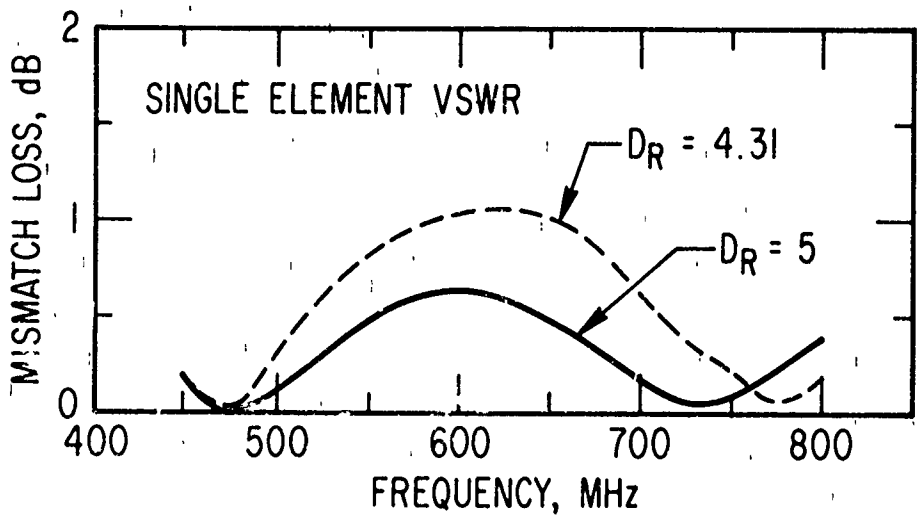

Figure 14. Mismatch Losses for 4.31- and 5-in. Dipole-to-Reflector Spacings

3. RADIATION PATTERNS

Radiation patterns of the 3 × 3 array were measured for an element spacing of 16 in., with dipole-to-reflector spacings of 4.31 and 5 in., and for an element spacing of 18 in. with a 5-in. dipole-to-reflector spacing. A summary of the computed and measured pattern characteristics is presented in this section.

Until a circularly polarized transmitting antenna was made available for the array radiation pattern measurements, a 6-ft parabolic reflector with a rotating linearly polarized dipole feed was used as an illuminating source. With the rotating linearly polarized source, the axial ratio can be determined for any aspect angle. The pattern response to a circularly polarized wave can then be determined by taking the RMS value of the maximum and minimum signals for a given angle:

$$E_{cp} = \sqrt{\frac{E_{max}^2 + E_{min}^2}{2}}$$

By using this RMS technique, the measured circularly polarized response was established, and the principal radiation characteristics such as beamwidth, EOE correction factors, and sidelobe levels were compared with the computed values and with the measured patterns for a circularly polarized source.

Figure 15 shows representative patterns recorded with both a rotating linearly polarized and a circularly polarized source for 450, 500, 600, 700, and 800 MHz. These patterns are for an element spacing of 16 in. and a dipole-to-reflector spacing of 4.31 in. The distance between the transmitting and receiving antennas was approximately 60 ft. Only the patterns in the $\phi = 0$ deg plane (in the plane containing a row or column of elements) are shown, since this plane has the most pertinent information for comparison with the computed results. The $\phi = 45$ deg plane pattern has approximately the same beamwidth as the $\phi = 0$ deg plane, but the sidelobe levels are less than -20 dB as shown by the computed patterns and confirmed by the measured patterns. One $\phi = 45$ deg plane measured pattern for 450 MHz is shown in Fig. 15(b).

Figure 16 shows the measured patterns of the main lobe region (expanded abscissa, ±30 deg) taken with the rotating linearly polarized source. The element spacing was 16 in., and the dipole-to-reflector spacing was 5 in. The half-power beamwidth, EOE correction factor, and axial ratio can be accurately determined by using the expanded patterns.

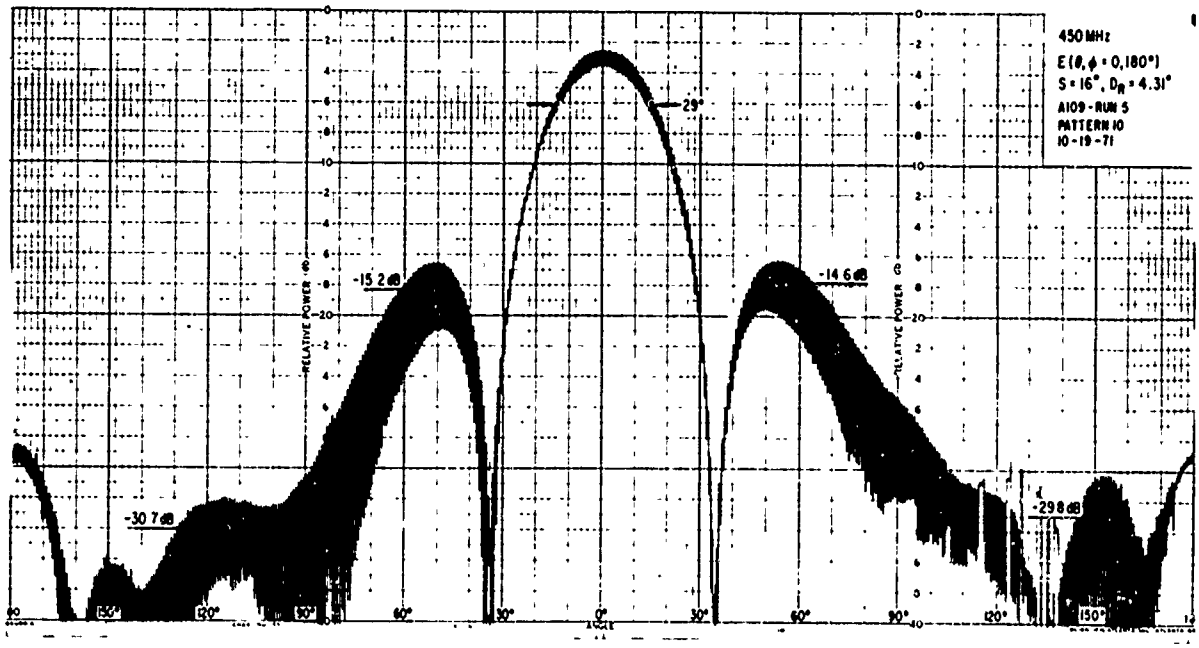

(a) 450 MHz, Rotating Linear Polarization

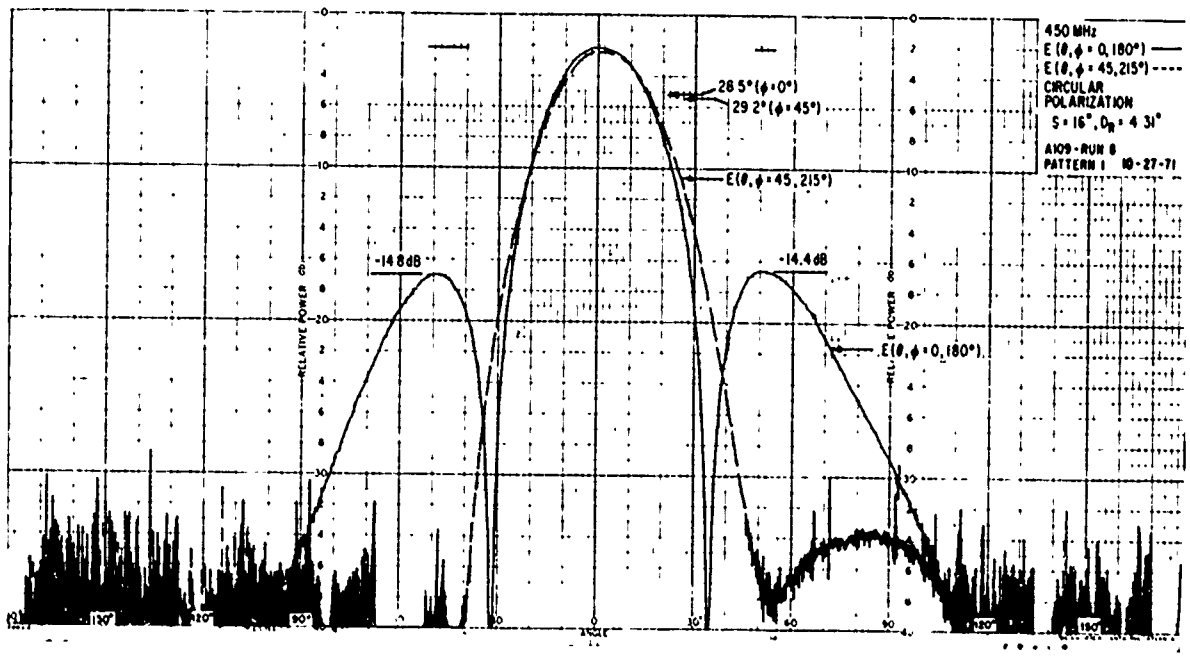

(b) 450 MHz, Circular Polarization

Figure 15. (Sheet 1 of 5) Measured Radiation Patterns for Element Spacing of 16 in. and Dipole-to-Reflector Spacing of 4.31 in. with Rotating Linearly Polarized and Circularly Polarized Illumination

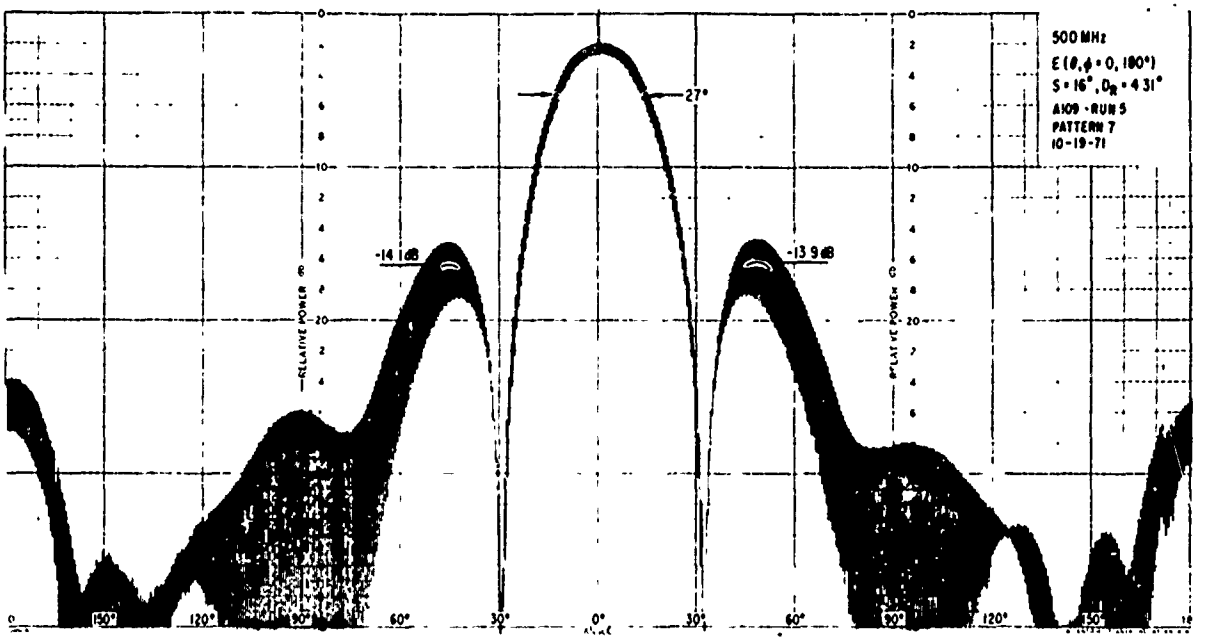

(c) 500 MHz, Rotating Linear Polarization

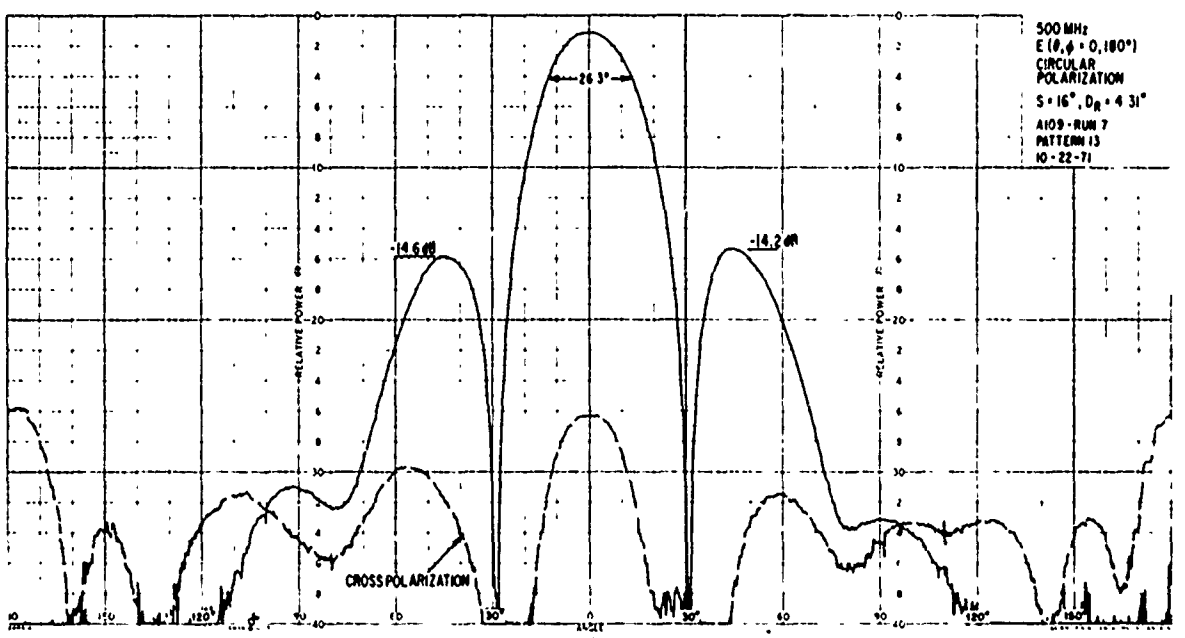

(d) 500 MHz, Circular Polarization

Figure 15. (Sheet 2 of 5) Measured Radiation Patterns for Element Spacing of 16 in. and Dipole-to-Reflector Spacing of 4.31 in. with Rotating Linearly Polarized and Circularly Polarized Illumination

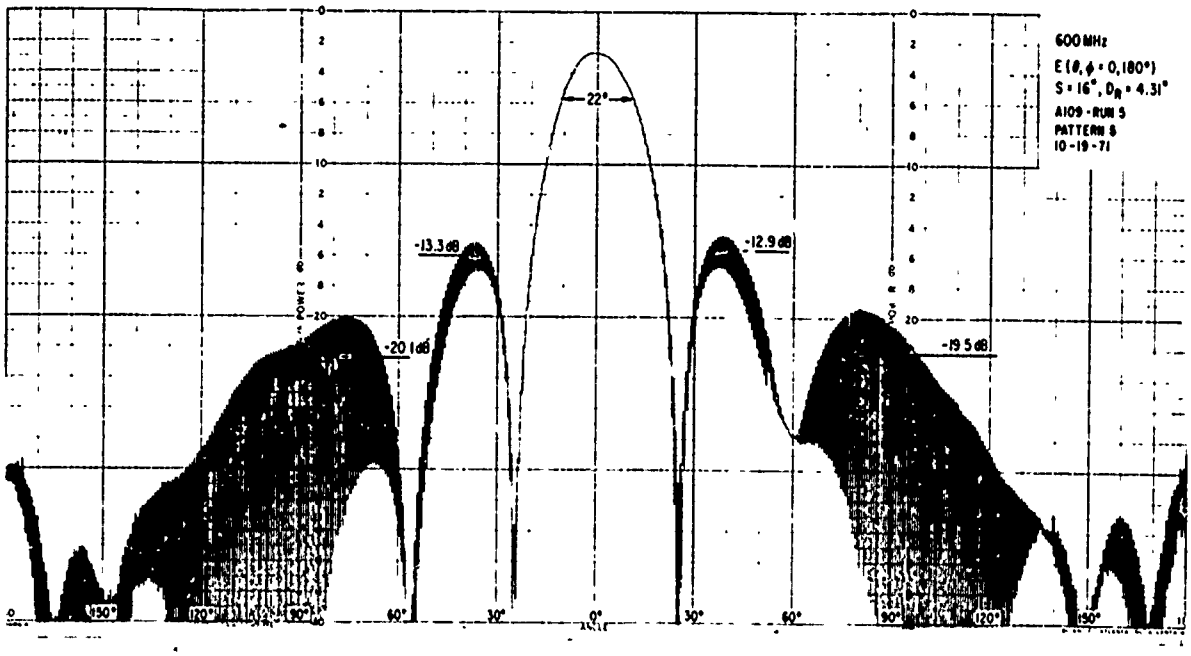

(e) 600 MHz, Rotating Linear Polarization

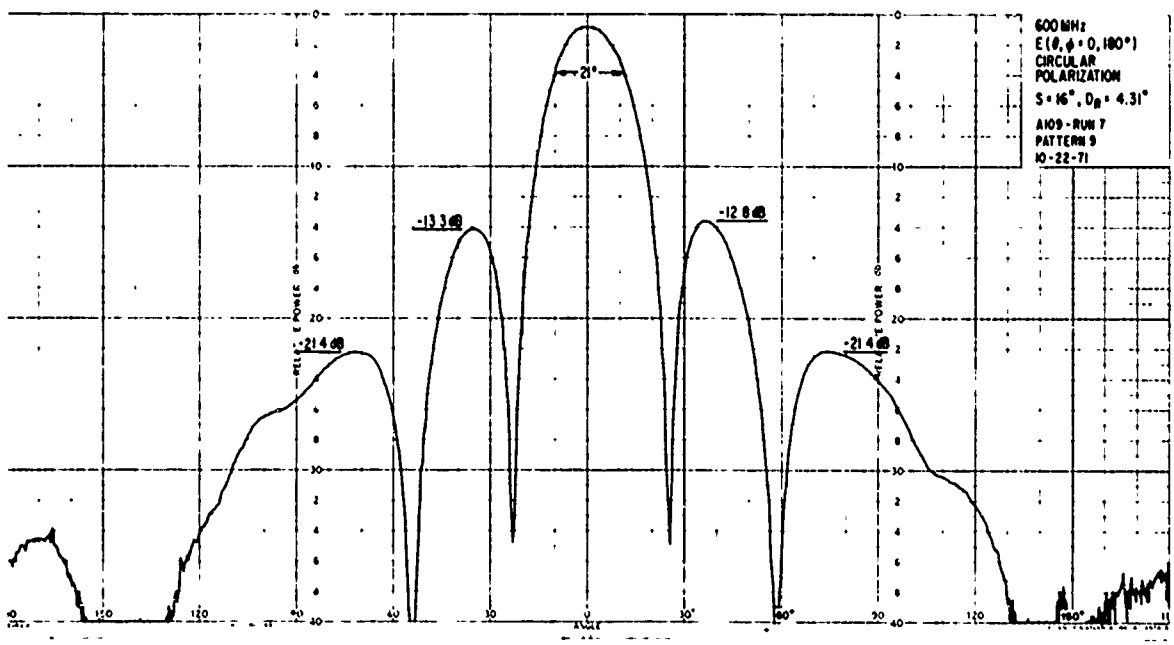

(f) 600 MHz, Circular Polarization

Figure 15. (Sheet 3 of 5) Measured Radiation Patterns for Element Spacing of 16 in. and Dipole-to-Reflector Spacing of 4.31 in. with Rotating Linearly Polarized and Circularly Polarized Illumination

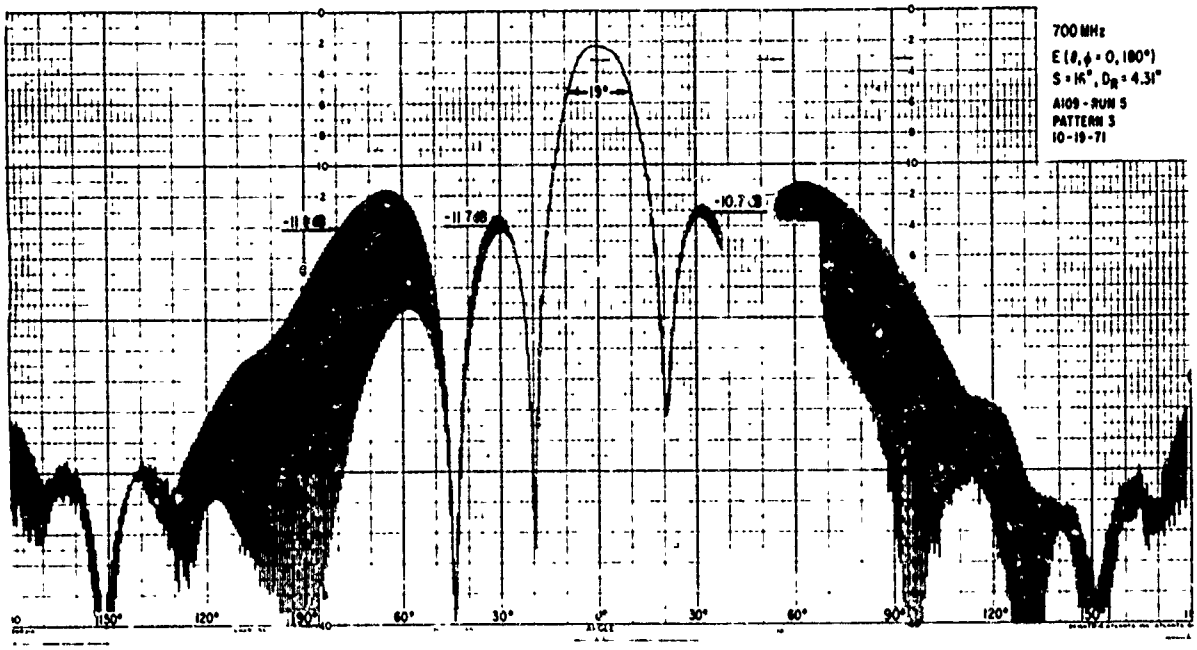

(g) 700 MHz, Rotating Linear Polarization

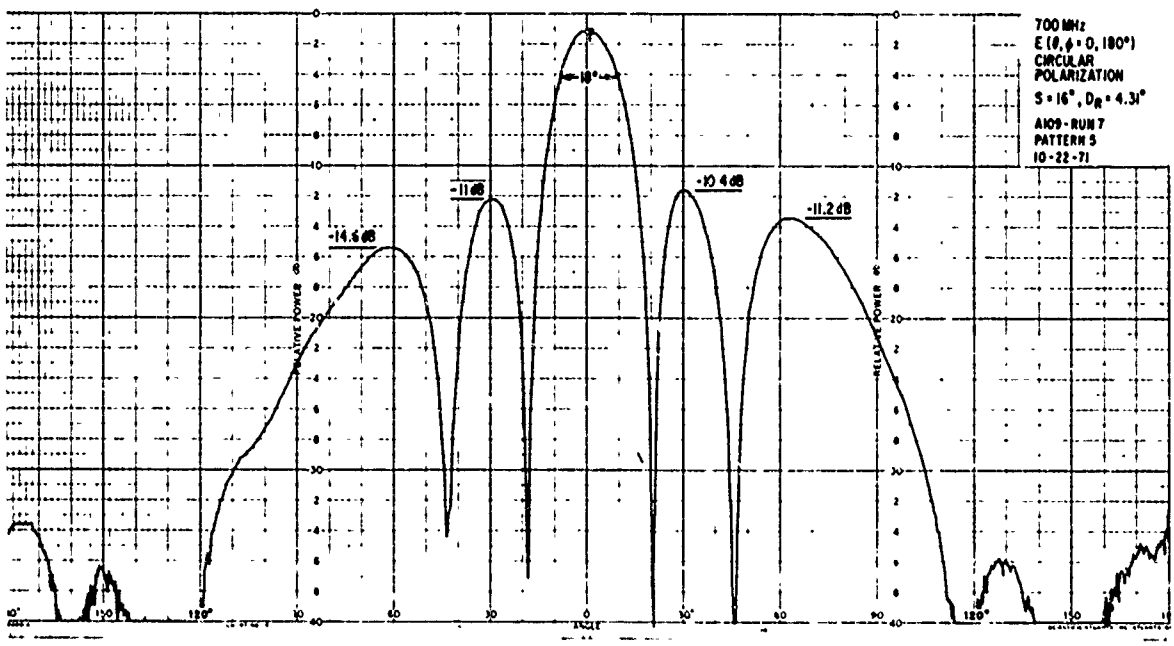

(h) 700 MHz, Circular Polarization

Figure 15. (Sheet 4 of 5) Measured Radiation Patterns for Element Spacing of 16 in. and Dipole-to-Reflector Spacing of 4.31 in. with Rotating Linearly Polarized and Circularly Polarized Illumination

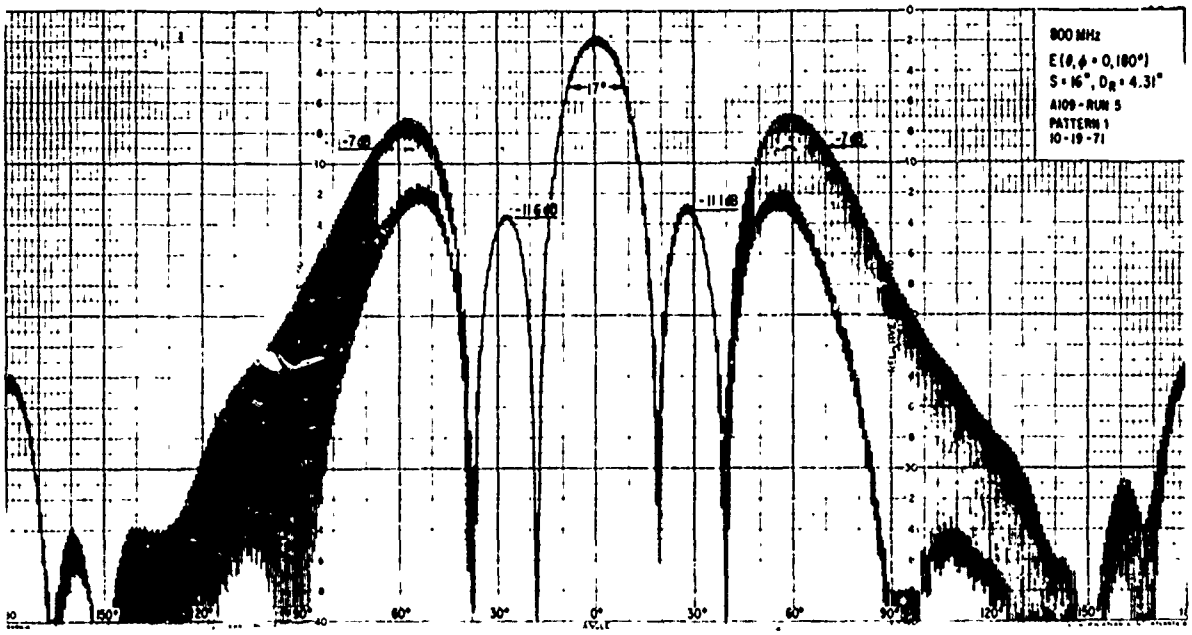

(i) 800 MHz, Rotating Linear Polarization

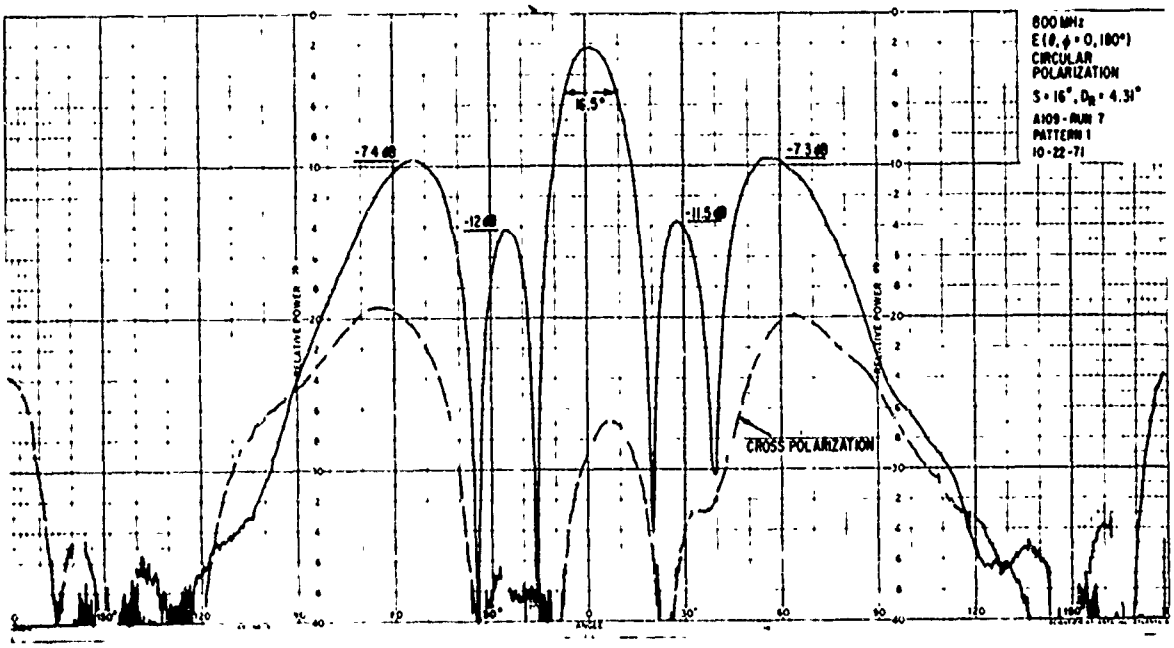

(j) 800 MHz, Circular Polarization

Figure 15. (Sheet 5 of 5) Measured Radiation Patterns for Element Spacing of 16 in. and Dipole-to-Reflector Spacing of 4.31 in. with Rotating Linearly Polarized and Circularly Polarized Illumination

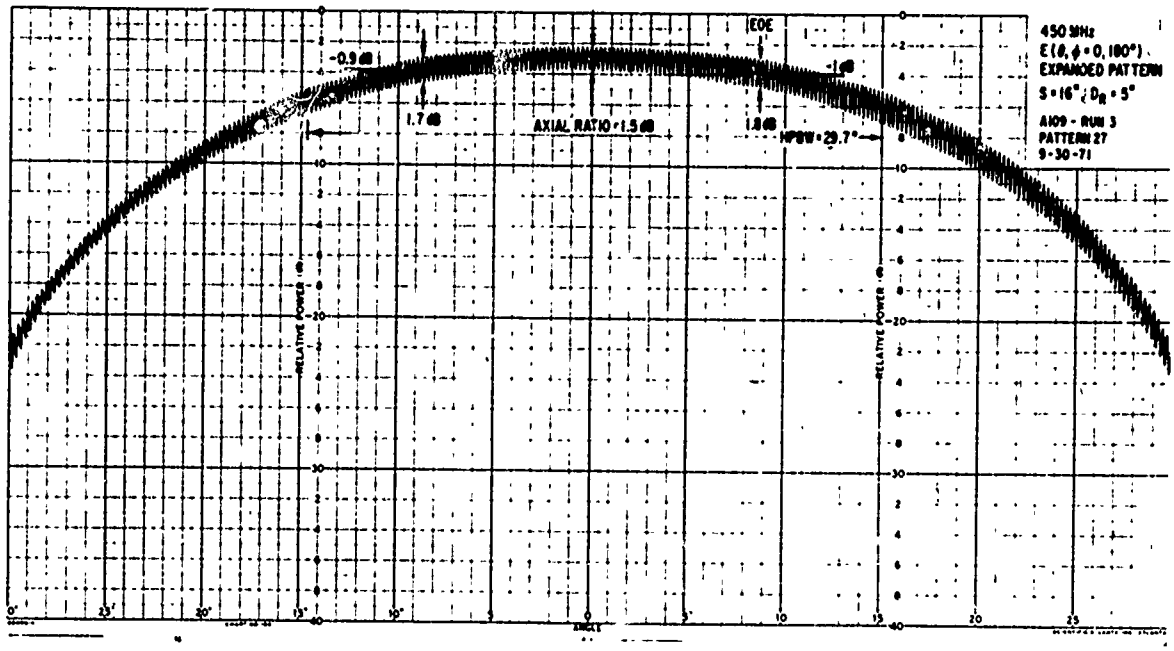

(a) 450 MHz

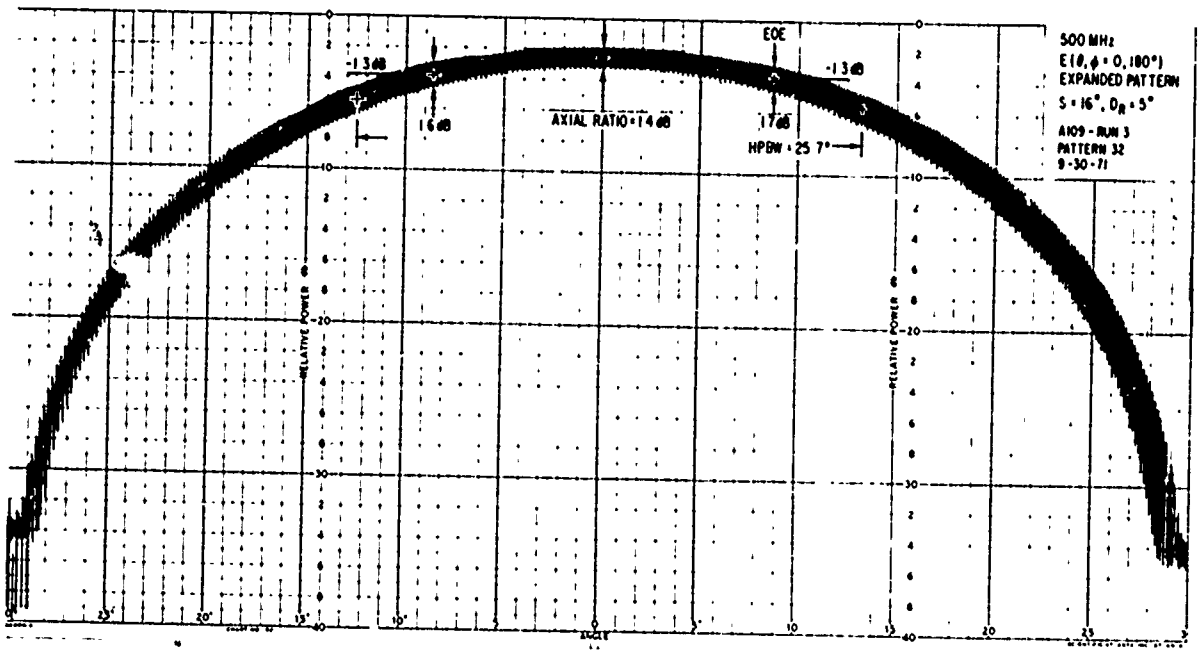

(b) 500 MHz

Figure 16. (Sheet 1 of 3) Measured Radiation Patterns with Expanded Abscissa Scale, Using a Rotating Linearly Polarized Source

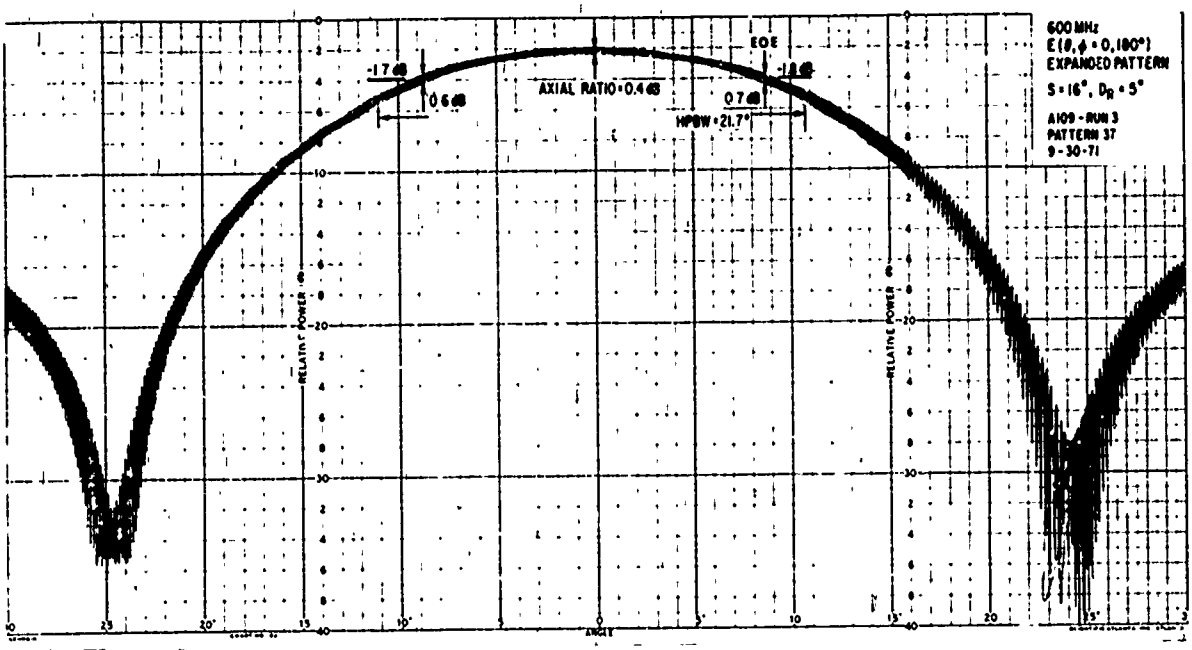

(c) 600 MHz

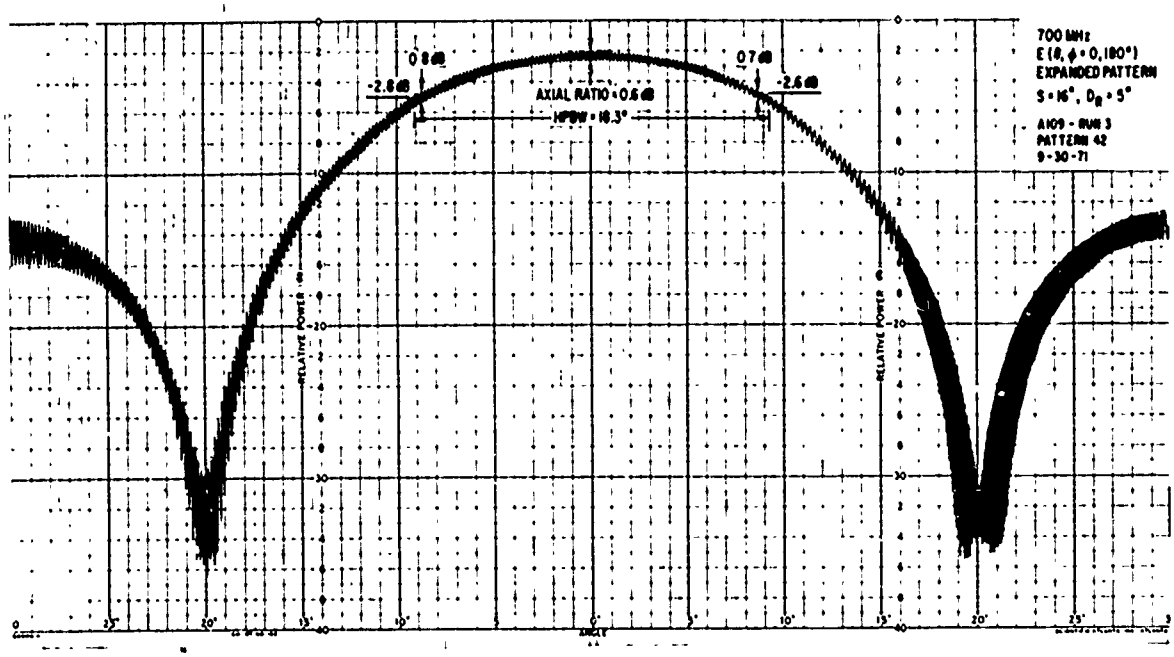

(d) 700 MHz

Figure 16. (Sheet 2 of 3) Measured Radiation Patterns with Expanded Abscissa Scale, Using a Rotating Linearly Polarized Source

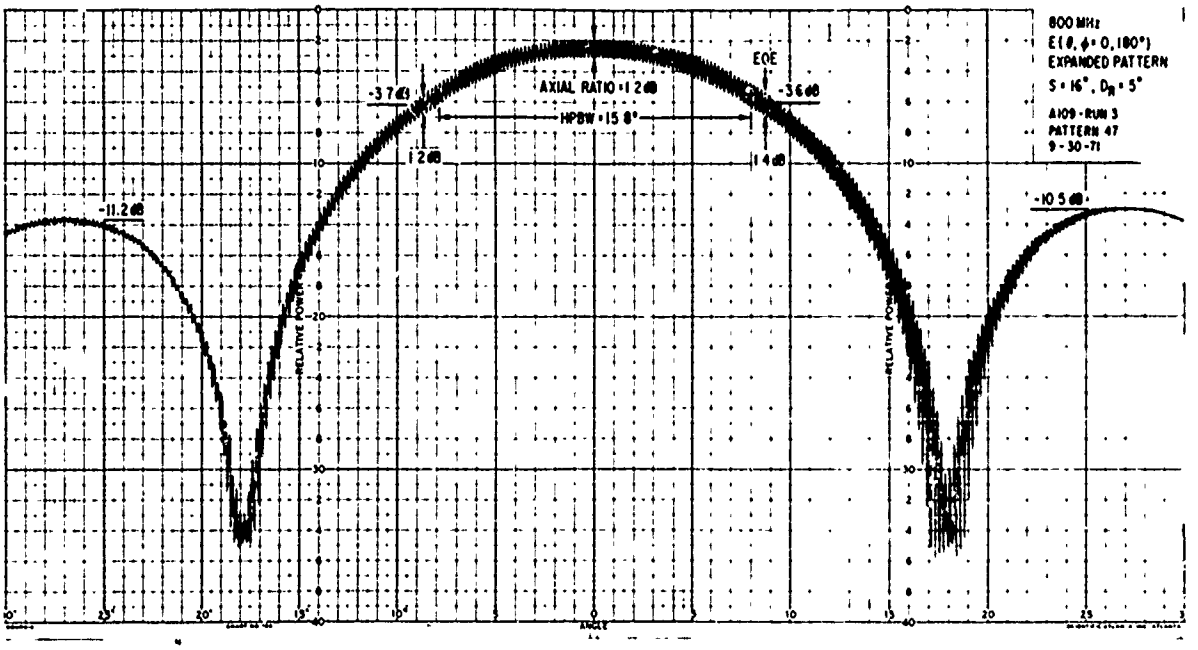

(e) 800 MHz

Figure 16. (Sheet 3 of 3) Measured Radiation Patterns with Expanded Abscissa Scale, Using a Rotating Linearly Polarized Source

A summary of the measured half-power beamwidths (HPBW), EOE (θ = 8.65 deg) correction factors, angles to the first null, and sidelobe levels is shown in Figs. 17, 18, and 19 for 3 array configurations, as follows:

Figure	Dipole-to-Reflector Spacing (D_r), in.	Element Spacing (s), in.
17	5.00	16
18	4.31	16
19	4.31	18

Comparisons are also made in these figures with the computed patterns. The measured values represent the average of several patterns. Since the computed HPBW and EOE correction factors for the ϕ = 0 and 45 deg planes are essentially the same, only the values for the ϕ = 0 deg plane are plotted. The HPBW in the ϕ = 45 deg plane is approximately 1% wider, while the EOE correction factor in the ϕ = 0 deg plane is slightly worse than the ϕ = 45 deg plane (differential less than 0.05 dB). The HPBW and EOE experimental data points for both principal planes compare very well with the predicted values, as shown in the summary curves. Also, there is a good correspondnece between the computed and measured first null positions in the ϕ = 0 deg plane, and the measured sidelobe levels are comparable to the computed levels.

4. DIRECTIVITY AND GAIN

A complete set of radiation patterns was taken for an element spacing of 16 in. with a dipole-to-reflector spacing of 5 in. and another set for s = 18 and D_r = 4.31 in. The purpose of these measurements was to determine the directivity by integration of the measured patterns. Great circle pattern cuts were taken in the ϕ = 0, 11.25, 22.5, 33.75, and 45 deg planes for frequencies of 450, 500, 600, 700, and 800 MHz. The measured directivities are compared with the computed values as shown in Fig. 20. For the

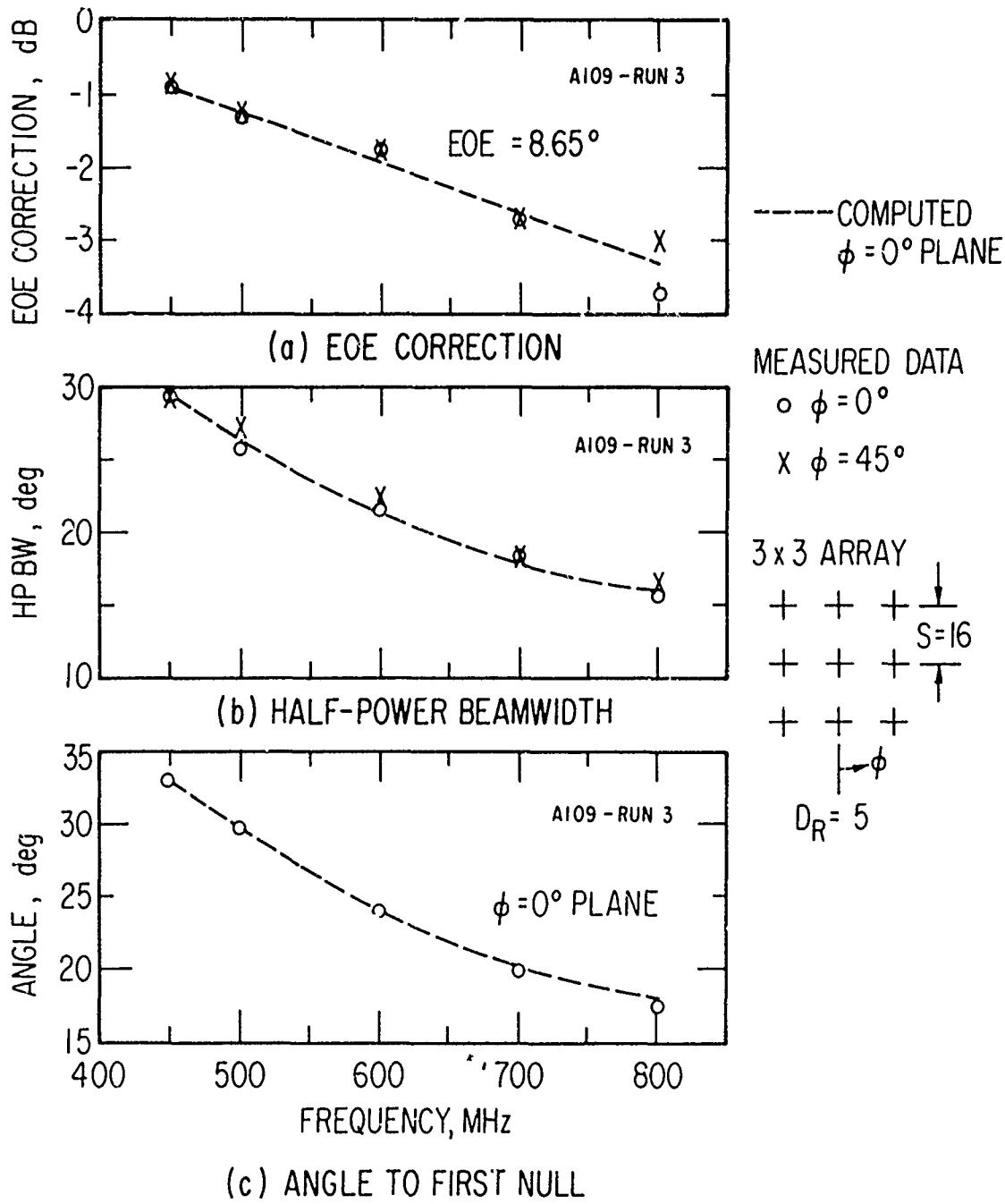

Figure 17. (Sheet 1 of 2) Comparison of Measured and Computed Radiation Pattern Characteristics for Element Spacing of 16 in. and Dipole-to-Reflector Spacing of 5 in.

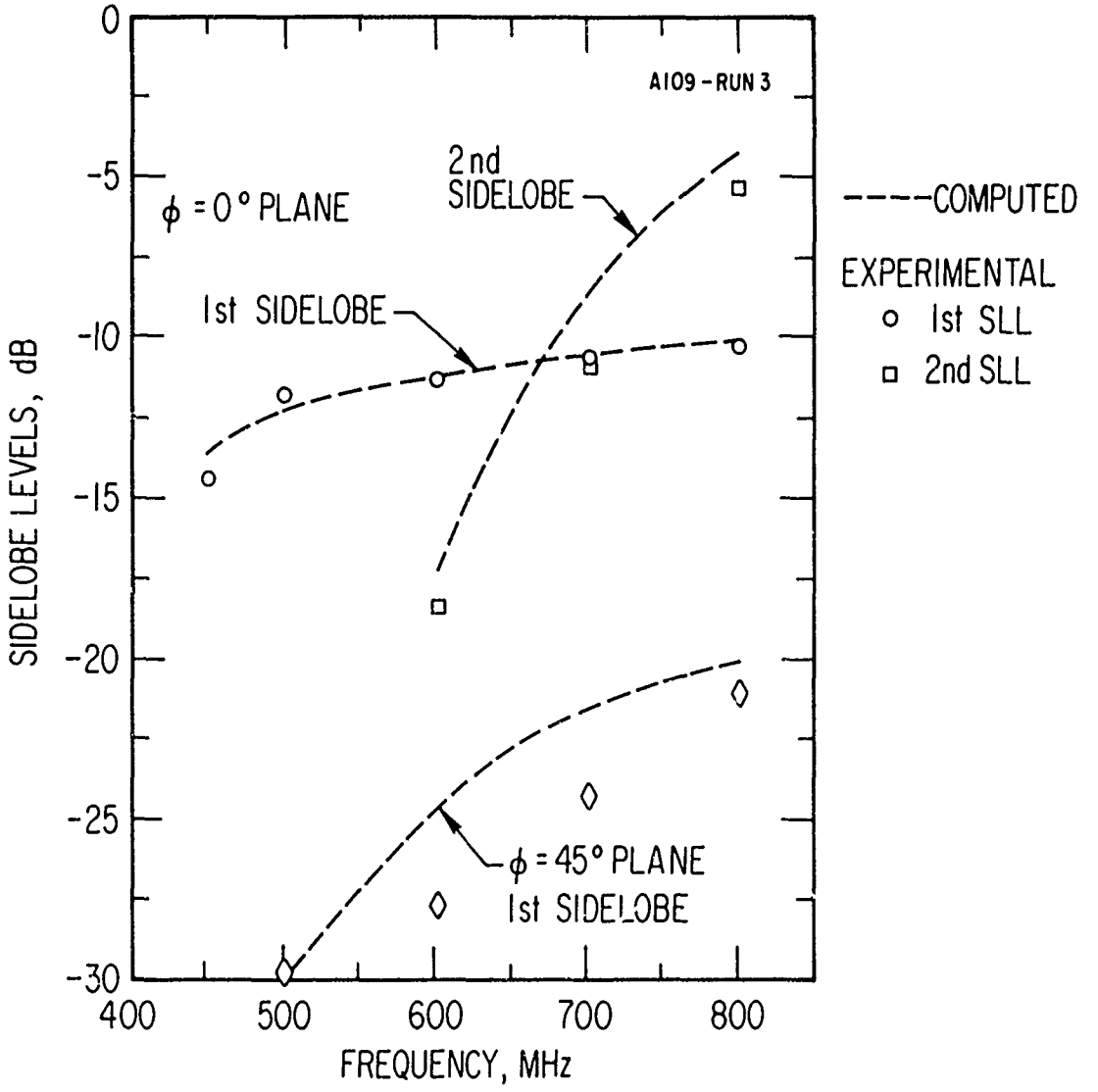

(d) FIRST AND SECOND SIDELOBE LEVELS

Figure 17. (Sheet 2 of 2) Comparison of Measured and Computed Radiation Pattern Characteristics for Element Spacing of 16 in. and Dipole-to-Reflector Spacing of 5 in.

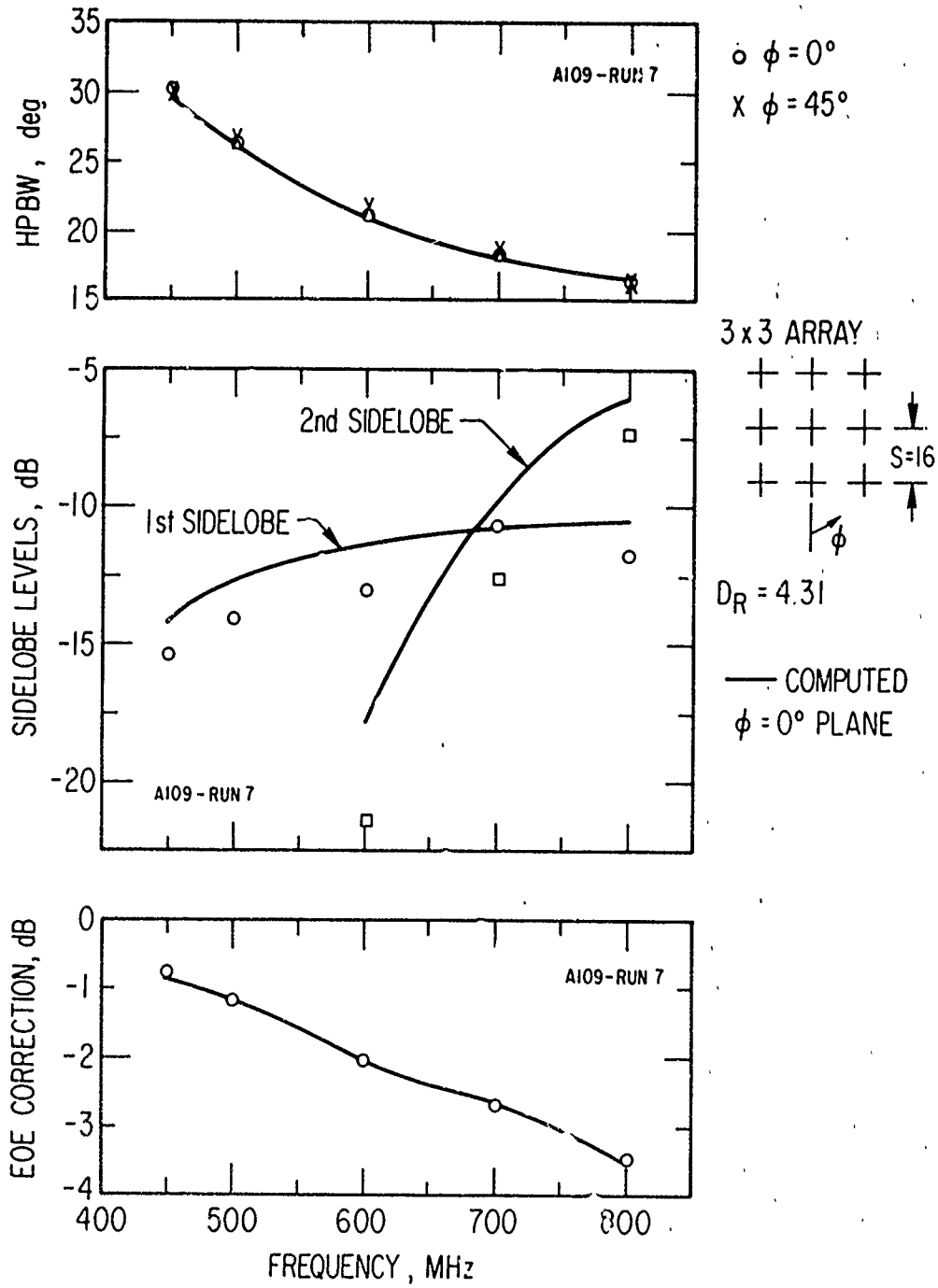

Figure 18. Comparison of Measured and Computed Radiation Pattern Characteristics for Element Spacing of 16 in. and Dipole-to-Reflector Spacing of 4.31 in.

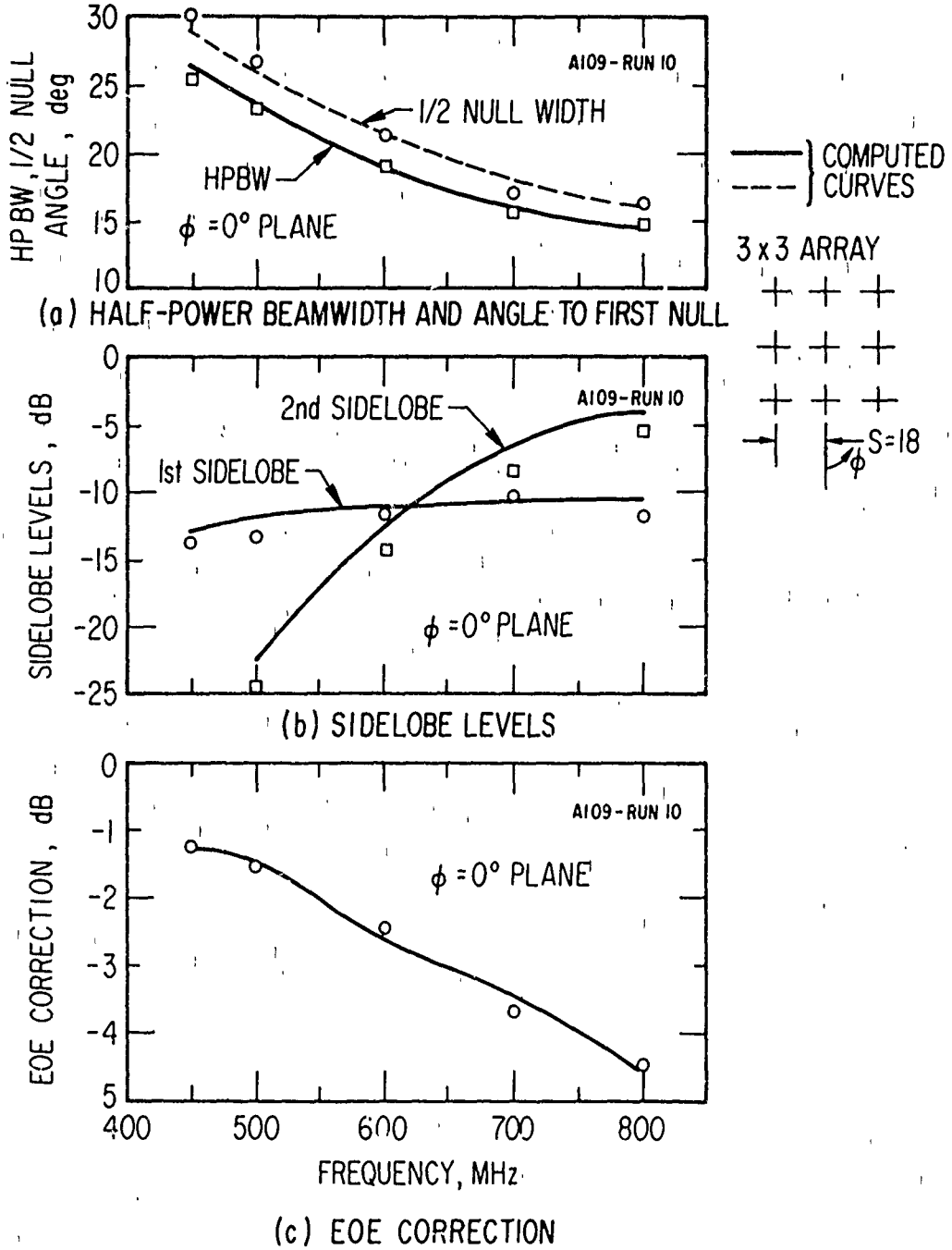

Figure 19. Comparison of Measured and Computed Radiation Pattern Characteristics for Element Spacing of 18 in. and Dipole-to-Reflector Spacing of 4.31 in.

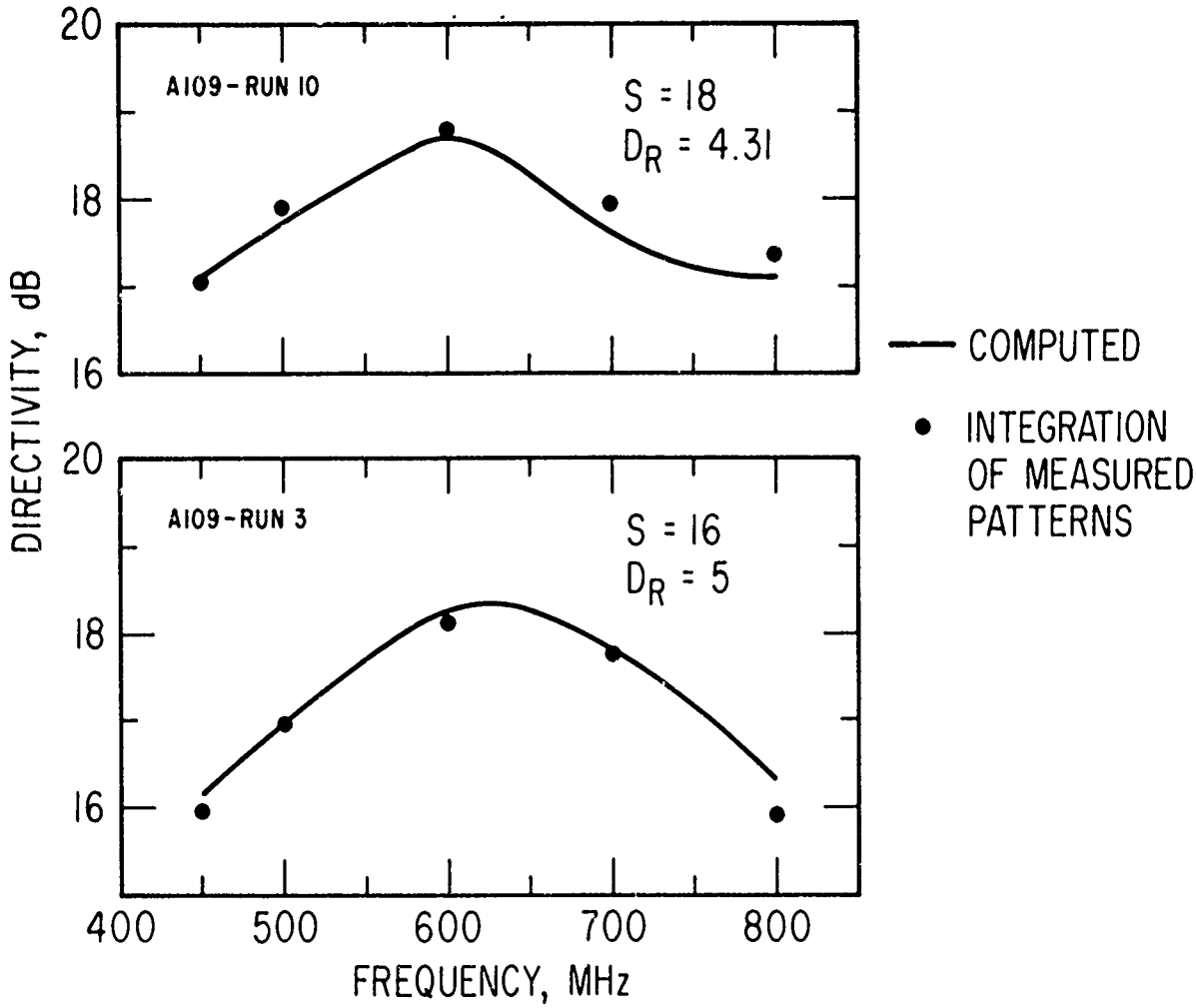

Figure 20. Comparison of Directivity Determined from Computed Patterns and Measured Patterns for the Planar Array

s = 16, D_r = 5 case, a linearly polarized rotating dipole was used in the pattern measurements, and the circularly polarized response was determined by taking the RMS value at each angle. For the second set of patterns, a circularly polarized source was used. The computed directivities are shown in Fig. 10, as determined from the array pattern using the measured isolated element patterns.

The predicted gains for the three array configurations tested (s = 16, D_r = 5; s = 16, D_r = 4.31; and s = 18, D_r = 4.31) were computed by using the theoretical directivities of Fig. 10 and subtracting the mismatch (Fig. 14) and the measured feed network losses (Fig. 11). Figure 21 shows plots of the predicted peak gain curves as well as the measured data points. The dotted line is the least squares fit of the measured data, with the standard deviation designated by s_d. The measured EOE gain curve is the peak gain less the computed EOE correction factor (Figs. 17, 18, and 19).

The correspondence between the measured and predicted gain values is good in certain portions of the band, and the maximum spread is as much as 1.2 dB. The average differences between the computed and measured gains are as follows:

Element Spacing (s), in.	Dipole-to-Reflector Spacing (D_r), in.	Difference Between Computed and Measured Gains, dB
16	5.00	0.18
16	4.31	0.18
18	4.31	0.63

As an average, the computed gain is approximately 0.33 dB higher than the measured gain over the operating frequency band.

The gain measurements were made by the substitution method, using a ridged waveguide horn* as a reference antenna. Each data point represents the average of six measurements. The procedure involves setting the transmitting antenna to vertical polarization. The array is then pointed to acquire

*The horn (NURAD, Inc., Model No. 7 RH) was calibrated in-house with a standard deviation of 0.25 dB by using both the two- and three-antenna methods.

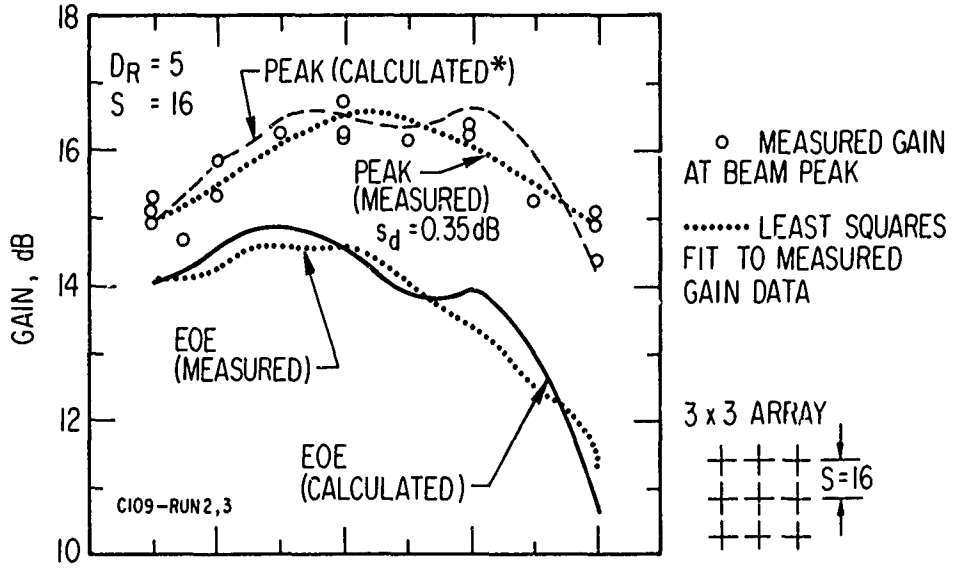

(a) DIPOLE-TO-REFLECTOR SPACING = 5 in., ELEMENT SPACING = 16 in.

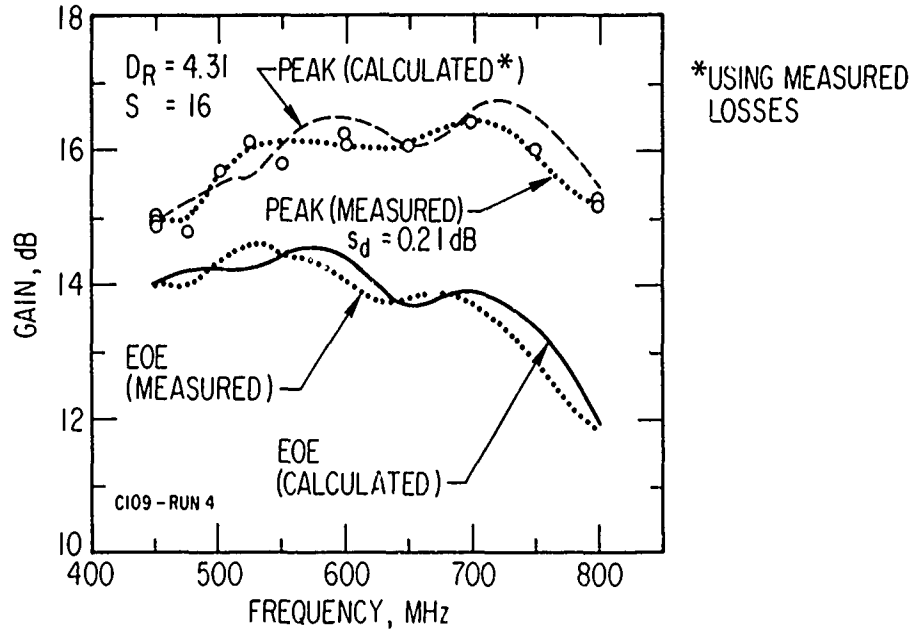

(b) DIPOLE-TO-REFLECTOR SPACING = 4.31 in., ELEMENT SPACING = 16 in.

Figure 21. (Sheet 1 of 2) Comparison of Measured and Predicted Gain for Three Planar Array Configurations

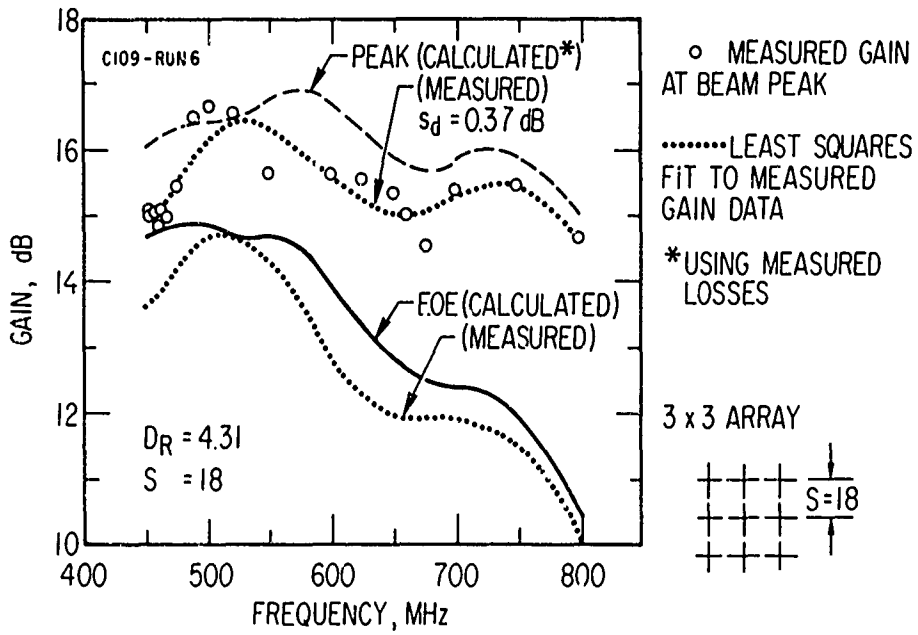

(c) DIPOLE-TO-REFLECTOR SPACING = 4.31 in., ELEMENT SPACING = 18 in.

Figure 21. (Sheet 2 of 2) Comparison of Measured and Predicted Gain for Three Planar Array Configurations

the maximum signal. The "head" of the antenna mount is rotated so that the maximum or minimum of the polarization ellipse is found. Three readings are taken as a function of range for the array at both the maximum and minimum of the polarization ellipse. Next, the horn is physically substituted for the array, and readings are made at the same corresponding range. The differential readings between the array and the horn are then used to calculate the measured gain. The correction factor from the axial ratio must also be used to convert the gain with respect to a circularly polarized wave; thus, the gain is referred to the RMS readings of the maximum and minimum of the polarization ellipse. The procedure is repeated for horizontal polarization, thus providing a total of six readings.

5. AXIAL RATIO

The axial ratio of the array may be determined from the gain measurements by taking the ratio of the maximum-to-minimum of the polarization ellipse. The average of the six readings for both the vertical and horizontal polarization measurements represents one data point in the axial ratio plots of Fig. 22.

The dotted curve in Fig. 22 is the power imbalance between the two output ports of the 90 deg hybrid.* The cross marks represent the measured power imbalance between the X and Y dipole ports of the feed network. The data indicate that the axial ratio is primarily determined by the power split of the hybrid, while the feed network and dipoles cause only negligible deterioration of the axial ratio. Based on the three sets of axial ratio measurements, the maximum deviation with respect to the power imbalance of the hybrid outputs is 0.9 dB, and, as an average, the deviation is less than 0.1 dB over the operating frequency band.

Figure 22 depicts the axial ratio at the beam peak. The axial ratio at EOE can be established from the expanded-abscissa patterns of Fig. 16, which show the relative axial ratios throughout the main lobe. The increase in axial ratio at the EOE angle over the beam peak is generally less than 0.3 dB.

*Designed for 500 to 1000 MHz operation.

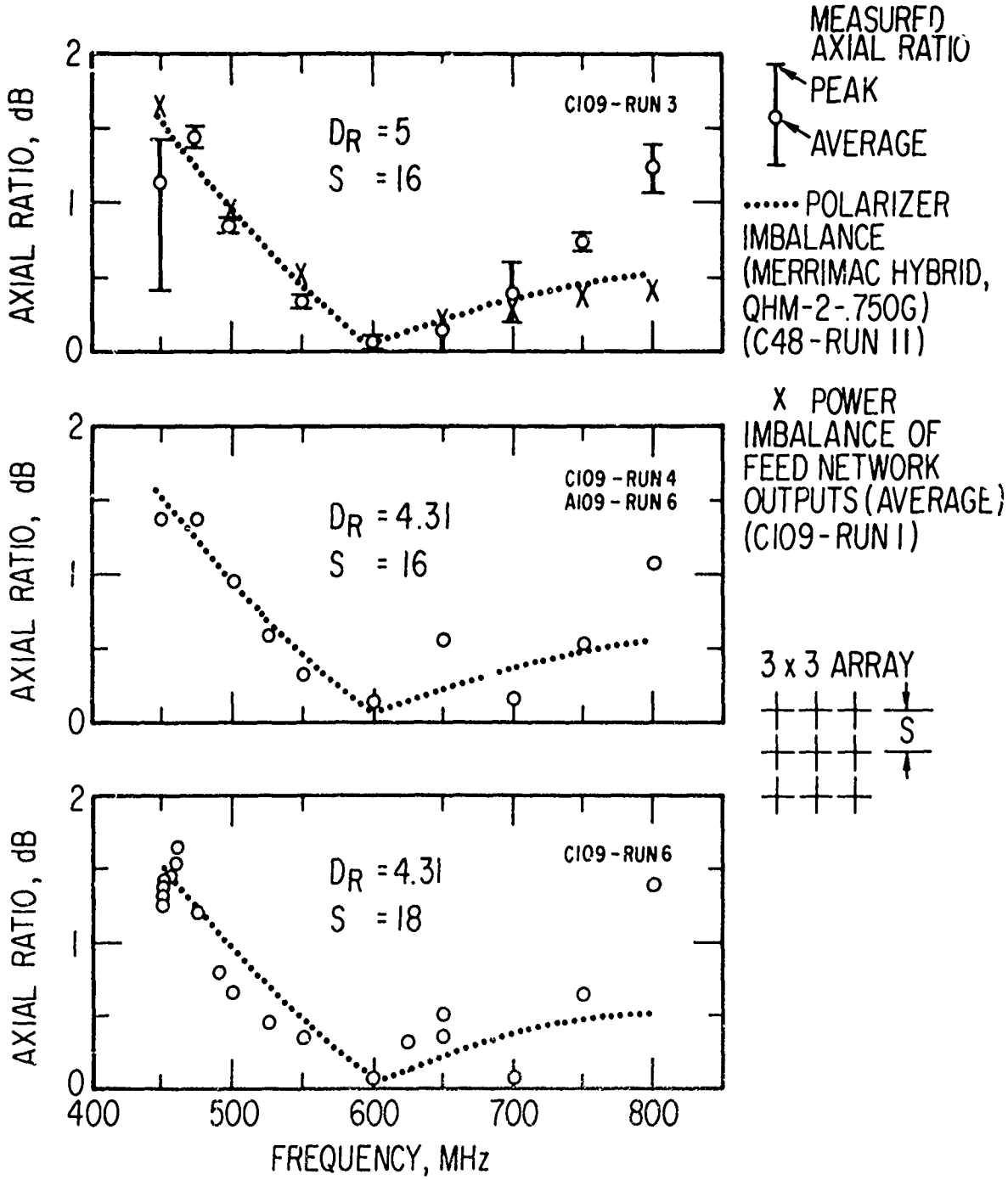

Figure 22. Measured Axial Ratios at the Beam Peak for Three Planar Array Configurations

IV. SUMMARY AND CONCLUSIONS

A half-scale model of a planar array intended for use on a synchronous satellite was constructed and tested over the 450 to 800 MHz frequency range (225 to 400 MHz full-scale). The array consists of nine (3 × 3 configuration) crossed open-sleeve dipole elements mounted on a 52-in. square reflector. The array elements are uniformly excited in order to maximize the antenna gain. The basic radiating element has relatively good VSWR response and pattern characteristics over the 1.8:1 frequency band. The VSWR of the array looking into the power divider input ports of the X and Y dipole elements is less than 2.8:1 and 2.3:1 for dipole-to-reflector spacings of 4.31 and 5 in. (half-scale), respectively. With further optimization, i.e., by varying the dipole and sleeve parameters, the VSWR response can be improved.

Comparisons were made between the computed and measured results, and relatively good correlation was observed. The calculations were performed using the conventional $\frac{\sin Nx}{N \sin x}$ array factor and a measured element pattern of a single isolated crossed dipole mounted on the center of a 52-in. square reflector. By integration of the measured array patterns, the directivities obtained compare very well with the predicted values over the entire frequency band. However, the measured gain as an average over the frequency band was 0.33 dB lower than the predicted gain values. It is shown that the antenna can provide an EOE gain (gain in the direction of the edge-of-the-earth, or ±8.65 deg from the nadir) of greater than 14 dB from 225 to 250 MHz, and greater than 11 dB from 250 to 400 MHz, based on the results of the half-scale model measurements and also using the component losses associated with the scaled frequencies.

The measured on-axis axial ratio of the array is less than 1.6 dB throughout the entire frequency band. However, the axial ratio of the array was found to be determined primarily from the power imbalance between the two output ports of the 90-deg hybrid that was used as the polarizer; i.e., the effects of the feed network and the dipoles did not significantly affect the axial

ratio. Based on the measurements, the maximum axial ratio deviation due to the power imbalance of the hybrid outputs is 0.9 dB, and, as an average, the deviation is less than 0.1 dB. Thus, if a hybrid is designed for the frequency band of interest, the axial ratio would be less than the values reported here. The increase in EOE axial ratio is less than 0.3 dB from the value at beam peak.

REFERENCES

1. H. E. King and J. L. Wong, "An Experimental Study of a Balun-Fed, Open-Sleeve Dipole in Front of a Metallic Reflector," IEEE Trans. Antennas and Propagation AP-20, 201-204 (March 1972).

2. H. E. King and J. L. Wong, 225 to 400 MHz Antenna for Spin-Stabilized Synchronous Satellites, Technical Report TR-0172(2162)-1, The Aerospace Corporation, El Segundo, Calif. (Jan. 1972).

3. E. L. Bock, J. A. Nelson, and A. Dorne, "Sleeve Antennas," Very High Frequency Techniques, ed. H. J. Reich, Radio Research Laboratory, Harvard University, McGraw-Hill Book Co., New York (1947) p. 123.

4. H. B. Barkley, The Open-Sleeve as a Broadband Antenna, TR No. 14, U.S. Naval Postgraduate School, Monterey, Calif. (June 1955), DDC AD 82 036.